Neuroscience 203 (2012) 59–77

SUBPOPULATIONS OF NEUROKININ 1 RECEPTOR-EXPRESSING NEURONS IN THE RAT LATERAL AMYGDALA DISPLAY A DIFFERENTIAL PATTERN OF INNERVATION FROM DISTINCT GLUTAMATERGIC AFFERENTS

H. K. SREEPATHI[1] AND F. FERRAGUTI*

Department of Pharmacology, Innsbruck Medical University, 6020 Innsbruck, Austria

Abstract—Substance P by acting on its preferred receptor neurokinin 1 (NK1) in the amygdala appears to be critically involved in the modulation of fear and anxiety. The present study was undertaken to identify neurochemically specific subpopulations of neuron expressing NK1 receptors in the lateral amygdaloid nucleus (LA), a key site for regulating these behaviors. We also analyzed the sources of glutamatergic inputs to these neurons. Immunofluorescence analysis of the co-expression of NK1 with calcium binding proteins in LA revealed that ~35% of NK1-containing neurons co-expressed parvalbumin (PV), whereas no co-localization was detected in the basal amygdaloid nucleus. We also show that neurons expressing NK1 receptors in LA did not contain detectable levels of calcium/calmodulin kinase IIα, thus suggesting that NK1 receptors are expressed by interneurons. By using a dual immunoperoxidase/immunogold-silver procedure at the ultrastructural level, we found that in LA ~75% of glutamatergic synapses onto NK1-expressing neurons were labeled for the vesicular glutamate transporter 1 indicating that they most likely are of cortical, hippocampal, or intrinsic origin. The remaining ~25% were immunoreactive for the vesicular glutamate transporter 2 (VGluT2), and may then originate from subcortical areas. On the other hand, we could not detect VGluT2-containing inputs onto NK1/PV immunopositive neurons. Our data add to previous localization studies by describing an unexpected variation between LA and basal nucleus of the amygdala (BA) in the neurochemical phenotype of NK1-expressing neurons and reveal the relative source of glutamatergic inputs that may activate these neurons, which in turn regulate fear and anxiety responses.

Key words: NK1 receptor, amygdala, interneuron, glutamate, parvalbumin.

[1] Present address: National Centre for Biological Sciences, Bangalore 560065, India.

*Corresponding author. Tel: +43-512-9003-71204; fax: +43-512-9003-73200.

E-mail address: francesco.ferraguti@i-med.ac.at (F. Ferraguti).

Abbreviations: BA, basal nucleus of the amygdala; BLA, basolateral complex of the amygdala; BP, band pass; CaMKIIα, calcium/calmodulin kinase IIα; CB, calbindin-D28K; CBP, calcium binding protein; CR, calretinin; DAB, 3,3′-diaminobenzidine; GAD67, glutamate decarboxylase isoform of 67 kDa; HRP, horseradish peroxidase; LA, lateral nucleus of the amygdala; LI, like immunoreactivity; NGS, normal goat serum; NK1, neurokinin 1; PBS, phosphate buffered saline; PV, parvalbumin; RT, room temperature; SP, substance P; TBS, tris-buffered saline; TBS-T, 0.1% v/v Triton X-100 in TBS; VGluT, vesicular glutamate transporter.

A growing body of evidence has shown that in the amygdala the neuropeptide substance P (SP) and its preferred receptor neurokinin 1 (NK1) modulate affective behavior and stress responses (Ebner and Singewald, 2006; Furmark et al., 2005; McLean, 2005). Focal injection into the basolateral complex of the amygdala (BLA) of SP conjugated to the toxin saporin resulted in the specific lesion of NK1-expressing neurons, and produced anxiogenic-like behavior in rodents (Gadd et al., 2003; Truitt et al., 2007, 2009). Conversely, injection of the NK1 selective antagonist L770735 reduced the amount of separation-induced vocalization in newborn guinea pigs (Boyce et al., 2001), consistent with the anxiolytic-like behavior observed in NK1-null mice (Santarelli et al., 2001).

A better knowledge of the neurons and circuitries containing NK1 receptors in the BLA, which is composed of the basal (BA), lateral (LA), and accessory basal nuclei, may help to reconcile these conflicting functional data. Activation of NK1 receptors in the guinea pig BA stimulated inhibitory synaptic activity (Maubach et al., 2001), thus suggesting that SP activates NK1 receptors localized on GABAergic interneurons within this amygdaloid area. However, NK1-like immunoreactivity (LI) was reported in a small number of putative pyramidal cells in the human BA (Maubach et al., 2001). Previous studies have shown that neurons bearing NK1 receptors in the rat BA lack parvalbumin (PV)- and calretinin (CR)-LI, but co-express calbindin-D28K (CB), neuropeptide Y, somatostatin, or cholecystokinin (Levita et al., 2003; Truitt et al., 2009). On the other hand, no detailed studies have investigated the neuronal localization of NK1 receptors in the LA.

In the BLA, nearly 85% of the neurons are glutamatergic pyramidal-like or projection neurons, whereas the remaining 15% are local interneurons (McDonald, 1984, 1992). In recent years, BA interneurons have been intensely studied and their specific content in calcium binding proteins (CBPs) and/or neuropeptides has been used to characterize the main subtypes (Mascagni et al., 2009; McDonald and Betette, 2001; McDonald and Mascagni, 2001; Spampanato et al., 2011). Interneurons expressing PV were shown to constitute ~40% of all GABAergic interneurons in the BLA (McDonald and Mascagni, 2001; Smith et al., 1998; Sorvari et al., 1995) and to be entirely separated from those containing CR (Kemppainen and Pitkänen, 2000), whereas a large proportion (~80%) of PV-containing neurons co-expressed CB (McDonald and Betette, 2001). On the other hand, much fewer studies

0306-4522
doi:10.1016/j.neuroscience.2011.12.006

have investigated the properties and subpopulations of interneurons in the LA (Sosulina et al., 2006, 2010).

The LA is one of the main targets in the amygdala for extrinsic glutamatergic inputs, mostly arising from the thalamus and the neocortex (LeDoux et al., 1990; Romanski and LeDoux, 1993; Sah et al., 2003). It is believed that these extrinsic inputs target both pyramidal-like cells and interneurons (Farb and Ledoux, 1999; Smith et al., 2000; Woodson et al., 2000). Although the innervation of LA interneurons by distinct excitatory inputs is likely of fundamental importance for determining the firing and synchronization of pyramidal-like neurons, little is known about this important issue.

Here, we have determined the pattern of co-localization of NK1-expressing neurons with calcium/calmodulin kinase IIα (CaMKIIα), glutamate decarboxylase isoform of 67 kDa (GAD67), or CBPs in the rat LA, and compared it with that in the BA. We have then analyzed quantitatively the glutamatergic synaptic innervation of distinct subclasses of NK1-immunopositive neurons in the LA by means of pre-embedding immunoelectron microscopy. Parts of these data have been previously presented in abstract form (Sreepathi and Ferraguti, 2008).

EXPERIMENTAL PROCEDURES

Materials

Thiopental was obtained from Biochemie (Kundl, Austria). Normal goat serum (NGS), biotinylated antibodies, and the avidin-biotinylated horseradish peroxidase complex were purchased from Vector Laboratories (Burlingame, CA, USA). Fab-fragments and antibodies coupled to gold particles as well as the HQ silver enhancement kit were from Nanoprobes (Stony Brook, NY, USA). Paraformaldehyde, glutaraldehyde, osmium tetroxide, and uranyl acetate were from Agar Scientific Ltd. (Stansted, UK). 3,3′ diaminobenzidine as well as all other chemicals were purchased from Sigma (Vienna, Austria).

Animals and tissue preparation

This study was carried out on adult male Sprague–Dawley rats (300–400 g; Department of Laboratory Animals and Genetics, Medical University Vienna, Vienna, Austria). A total of 15 rats have been used for this study, 10 for light microscopy and 5 for electron microscopy experiments. All experimental protocols were approved by the Austrian Animal Experimentation Ethics Board in compliance with both the European Convention for the Protection of Vertebrate Animals used for Experimental and Other Scientific Purposes (ETS no. 123) and the European Communities Council Directive of 24 November 1986 (86/609/EEC). The authors further attest that all efforts were made to minimize the number of animals used and their suffering. Animals were deeply anesthetized by intraperitoneal injection of thiopental (100 mg/kg, i.p.) and perfused transcardially with phosphate buffered saline (PBS; 0.9% NaCl, pH 7.4) followed by ice-cold fixative made of 4% w/v paraformaldehyde and 15% v/v of a saturated solution of picric acid in phosphate buffer (PB; 0.1 M, pH 7.4) for 15 min. For electron microscopy experiments glutaraldehyde (25%) at a final dilution of 0.05% v/v was added to the fixative just before the perfusion. Brains were immediately removed from the skull, washed in 0.1 M PB, and sliced coronally in 40 (for light microscopy) or 70 μm (for electron microscopy) thick sections on a Leica VT1000S vibratome (Leica Microsystems, Vienna, Austria). Sections were stored in 0.1 M PB containing 0.05% sodium azide at 6 °C until immunohistochemical experiments were performed.

Immunohistochemistry for light microscopy

Free-floating sections were first washed in tris-buffered saline (TBS; 0.9% NaCl, pH 7.4), incubated with 20% NGS and 0.1% v/v Triton X-100 in TBS (TBS-T) to block nonspecific binding sites, and then with rabbit (Chemicon, Temecula, CA, USA; 1:10,000) or guinea pig (Biotrend, Cologne, Germany; 1:3000) polyclonal anti-NK1 antibodies diluted in TBS-T containing 2% NGS, for 48 h at 6 °C. After three washes in TBS, biotinylated secondary antibodies (goat anti-rabbit IgG, cat. no. BA-1000 or goat anti-guinea pig IgG, cat. no. BA-7000, Vector Laboratories) were applied overnight at 6 °C at a dilution of 1:500 in a buffer with the same composition as for the primary antibody. The sections were then washed and incubated in the avidin-biotin–horseradish peroxidase (HRP) complex (diluted 1:100; Vector Laboratories) in TBS overnight at 6 °C. On the following day, the sections were washed in TB several times, preincubated with 3,3′-diaminobenzidine (DAB; 0.5mg/ml) for 5 min and then H_2O_2 was added to the solution at a final dilution of 0.003% for 3–6 min. Subsequently, the sections were extensively washed with TB, mounted onto gelatin-coated glass slides, air-dried, and then treated with graded ethanol (50%, 70%, 90%, 95%, and 100%) and butylacetate. Finally, they were coverslipped with Eukitt (Agar Scientific Ltd.). Analysis was performed under a Zeiss Axiophot microscope (Zeiss, Jena, Germany). Images were taken through an AxioCam camera (Zeiss) by means of the openlab software (version 5.5.0; Improvision, Coventry, UK). Whole images were contrast-adjusted, sharpened, and cropped in Photoshop (Adobe) without changing any specific feature within.

Double- and triple-immunofluorescence experiments

Immunofluorescence experiments were carried out according to previously published procedures (Ferraguti et al., 2004). Briefly, free floating sections were extensively washed with TBS, then incubated in blocking solution (20% NGS in TBS-T) for 2 h at room temperature (RT). Sections were subsequently kept in primary antibodies, in combination or alone (see Table 1), diluted in TBS-T and 2% NGS for ~72 h at 6 °C. Sections were then washed in TBS (three times for 10 min) and incubated overnight (6 °C) with appropriate secondary antibodies in TBS-T and 2% NGS (Table 1). When biotinylated secondary antibodies were used, sections were first incubated overnight at 6 °C with these antibodies. The next day, after extensive washes in TBS, sections were incubated again overnight in a solution containing streptavidin-AMCA diluted at 1:1000 (Vector Laboratories) as well as all the other appropriate fluorochrome-conjugated secondary antibodies made up in TBS-T and 2% NGS. Sections were then washed, mounted onto gelatin-coated slides, and coverslipped with Vectashield (Vector Laboratories).

Image acquisition and analysis

Immunofluorescence was analyzed using a Zeiss AxioImager M1 microscope with epifluorescence illumination equipped with the following filter blocks: Alexa350 (excitation filter band pass [BP] 357/50 nm; reflection short-pass filter 425 nm; emission filter BP 445/50 nm), Cy2/Alexa488 (excitation filter BP 480/40 nm; reflection short-pass filter 505 nm; emission filter BP 527/30 nm), and Cy3 (excitation filter BP 545/25 nm; reflection short-pass filter 570 nm; emission filter BP 605/70 nm). Images were displayed and analyzed by the Openlab software (version 5.5.0; Improvision). Images were acquired through an ORCA-ER CCD camera (Hamamatsu, Hamamatsu City, Japan). Brightness and contrast were adjusted for the whole frame with no part of the frame modified independently in any way. To make sure that a lack of co-localization between NK1- and CaMKIIα-LI was not because of

Table 1. List of the concentrations and combinations of primary and secondary antibodies

Primary antibody	Source	Antigen	Species	Dilution	Secondary antibody	Dilution	Combinations
Calbindin	Swant; cat. No. 300 Lot. No. 18 (F)	Chicken gut calbindin D-28 kDa	Mouse IgG1	1:30,000 -LM	Dnk anti-Ms Alexa488 (Invitrogen)	1:1000	b
					Gt anti-Ms Biotinylated (Vector)+Streptavidin-AMCA	1:500 1:1,000	d,e
Calretinin	Swant; cat. No.6B3 Lot. No. 010399	Recombinant human calretinin-22 kDa	Mouse ascites	1:10,000 -LM	Dnk anti-Ms Alexa488 (Invitrogen)	1:1000	f
CaMKII	Chemicon; cat. No. MAB8699 Lot. No. LV1377413	Purified type II CaM Kinase	Mouse IgG1	1:100 -EM	Gt anti-Ms nanogold (Nanoprobes)	1:100	A
				1:100 -LM	Dnk anti-Ms Alexa488 (Invitrogen)	1:1000	a
GAD67	Chemicon; cat. No.MAB5406	Recombinant GAD67 protein	Mouse IgG2	1:3,500 -LM	Dnk anti-Ms Alexa488 (Invitrogen)	1:1000	i
Neurokinin 1 receptor	Chemicon; cat. No. AB5060 Lot. No. 23030368 and 0512016863	Synthetic peptide aminoacid sequence (385–407) of the Cterminus of the rat NK1	Rabbit serum	1:10,000 -LM	Dnk anti-Rb Cy3 (Jackson)	1:400	a, b, c, d, f, h
				1:5,000 -EM	Gt anti-Rb Biotinylated (Vector)	1:100	A, B, C
					Gt anti-Rb nanogold (Nanoprobes)	1:400	D, E
Neurokinin 1 receptor	Biotrend; cat. No. NA4200	The peptide aminoacid sequence (393–407) of the Cterminus of the rat NK1	Guinea pig serum	1:3,000 -LM	Dnk anti-GP Cy3 (Jackson)	1:400	e, g
Parvalbumin	Synaptic Systems; cat. No. 195004 Lot. No. 195004/1	Recombinant full length rat parvalbumin	Guinea pig serum	1:7,000 -LM	Gt anti-GP Alexa488 (Invitrogen)	1:1000	d
Parvalbumin	Swant; cat. No. PV-28 Lot. No. 5.5	Rat muscle parvalbumin	Rabbit serum	1:20,000 -LM	Dnk anti-Rb Alexa488 (Invitrogen)	1:1,1000	e, g
Parvalbumin	Swant; cat. No. 235 Lot. No. 10–11 (F)	Carp muscles parvalbumin	Mouse IgG1	1:5,000 -LM	Dnk anti-Ms Alexa488 (Invitrogen)	1:1000	c
					Gt anti-Ms Biotinylated (Vector)+Streptavidin-AMCA	1:500 1:1000	h
				1:5,000 -EM	Gt anti-Ms Biotynilated (Vector)	1:100	E
Vesicular glutamate transporter 1	Chemicon; cat. No. AB5905 Lot. No. 23050127	Synthetic peptide from rat VGluT1 protein	Guinea pig serum	1:2500 -EM	Gt anti-GP nanogold (Nanoprobes)	1:100	B
Vesicular glutamate transporter 2	Chemicon; cat. No. AB5907 Lot. No. 23041014	Synthetic peptide from rat VGluT2 protein	Guinea pig serum	1:5000 -EM	Gt anti-GP nanogold (Nanoprobes)	1:100	C,E
Vesicular glutamate transporter 3	Chemicon; cat. No. AB5421 Lot. No. 23050673	Synthetic peptide from rat VGluT3 protein	Guinea pig serum	1:30,000 -LM	Gt anti-GP Alexa488 (Invitrogen)	1:1000	h

Capital letters indicate reactions for pre-embedding electron microscopy, whereas small letters indicate reactions for immunofluorescence.

Dnk, donkey; GP, guinea pig; Gt, goat; Ms, mouse; Rb, rabbit.

poor penetration of the antibody for CaMKIIα, this double reaction was also analyzed using an SP5 confocal microscope (Leica Microsystems, Wetzlar, Germany) equipped with an HCX PL APO CS 20.0×0.70 objective. Imaging was performed using the 488 nm argon laser line for Alexa488 and a 561 nm laser for Cy3. Fluorescence emission was detected from 493 to 550 nm (Alexa488) and 566–700 nm (Cy3) controlled by the LAS AF 2.4.1. acquisition software.

Immunocytochemistry for electron microscopy (pre-embedding)

Free floating sections were washed three times in 0.1 M PB, cryoprotected in 20% sucrose made in 0.1 M PB overnight at 6 °C. After removal of the sucrose, the sections were freeze-thawed twice to allow antibody penetration and then incubated in 20% NGS in TBS for 2 h at RT. After blocking, sections were exposed for ~72 h at 6 °C to primary antibodies (see Table 1) made up in a solution containing 2% NGS in TBS. After three washes in TBS, sections were incubated overnight at 6 °C with the appropriate secondary antibodies (Table 1). When a single primary antibody was used, it was visualized either by HRP or by nanogold–silver-enhanced reaction. When more than one primary antibody was used, one of them was visualized by nanogold–silver-enhanced reaction and the second was visualized by HRP reaction. Silver enhancement was always carried out first. After several washes with TBS, sections incubated with Fab fragment secondary antibodies coupled to nanogold (1.4 nm) were extensively washed in MilliQ water and followed by silver enhancement of the gold particles with the HQ kit (Nanoprobes) for ~10–12 min. Sections were then washed extensively in MilliQ water and then with TB. Sections processed for the HRP reaction were incubated in ABC complex (diluted 1:100; Vector Laboratories) made up in TB overnight at 6 °C and then washed in TB several times before the antigen/antibody complex was visualized with DAB (0.5 mg/ml) using 0.003% H_2O_2 as the electron donor for 5–6 min. Sections were subsequently washed with 0.1 M PB and treated with 2% OsO_4 in 0.1 M PB for 40 min at RT. After several washes with 0.1 M PB and then with MilliQ water, sections were contrasted with 1% uranyl-acetate in 50% ethanol for 30 min at RT, making sure they were protected from light. Sections were washed with MilliQ water followed by graded ethanol (50%, 70%, 90%, 100%) and propylene oxide at RT. Sections were then quickly transferred into weighting boats containing epoxy resin (durcupan ACM-Fluka, Sigma) and kept overnight at RT. The following day, the sections were transferred onto siliconized slides, coverslipped with ACLAR®-film coverslips (Ted Pella, Inc., Redding, CA, USA), and incubated for 3 days at 60 °C. Blocks containing specific nuclei of the amygdala were cut under a stereomicroscope and re-embedded in epoxy resin. Ultrathin sections (70 nm) were cut using a diamond knife (Diatome, Biel, Switzerland) on an ultramicrotome (Ultracut, Vienna, Leica), collected on copper slot grids coated with pioloform (Agar), and analyzed in a Philips CM120 electron microscope (Eindhoven, the Netherlands).

Antibody characterization and specificity of immunostainings

The monoclonal anti-calbindin D-28k antibody (Swant, Bellizona, Switzerland; Cat. no. 300; Lot. 18F) is a mouse IgG_1 produced by hybridization of mouse myeloma cells with spleen cells from mice immunized with calbindin D-28k purified from chicken gut. This monoclonal antibody stained the ^{45}Ca-binding spot of calbindin D-28k in a two-dimensional gel. The antibody reacts specifically with calbindin D-28k and does not cross-react with calretinin or other calcium binding proteins (manufacturer's technical information).

The anti-calretinin monoclonal antibody (Swant; Cat. no. 6B3, Lot. 010399) was raised in mouse by immunization with recombinant human calretinin-22k. Calretinin-22k is an alternative splice product of the calretinin gene and identical to calretinin up to Arg178. After fusion, hybridoma cells were screened with human recombinant calretinin as target, the clone 6B3 was selected, and ascites was produced. The antibody 6B3 recognizes an epitope within the first four EF-hands domains common to both calretinin and calretinin-22k. This antibody does not cross-react with calbindin-D28K or other known calcium-binding proteins, as determined by immunoblots (manufacturer's technical information).

The mouse monoclonal antibody to the alpha subunit of CaMKII (Chemicon; Cat. no. MAB8699, clone 6G9) was raised against purified type II CaMK. The specificity of this antibody, which recognizes both phosphorylated and nonphosphorylated forms of the kinase, has been well-documented in previous studies (Erondu and Kennedy, 1985). On Western blots, it produces a single band at 50 kDa.

The mouse monoclonal antibody to the glutamate decarboxylase 67 kDa isoform (Chemicon; Cat. no. MAB5406, clone 1G10.2) was raised against a recombinant GAD67 protein. The specificity of this antibody was assessed by the manufacturer on Western blots using SKNSH cell lysates and in immunocytochemistry on mouse somoatosensory cortex. Furthermore, this antibody detects on Western blot a band at the expected molecular weight of 67 kDa and does not cross-react with the GAD65 isoform on rat brain lysates (manufacturer's technical information).

The rabbit NK1 receptor antiserum (Chemicon; Cat. no. AB5060, Lot. 23030368 and 0512016863) was raised against the C-terminal 23 amino acids (residues 385–407) of the rat NK1 receptor. The immunostaining was abolished when the antibody was preabsorbed with an excess amount of C-terminal peptide (393–407) of NK-1 receptor (Piggins et al., 2001). Furthermore, the immunostaining in the rat brain was the same as that of a well-characterized rabbit polyclonal antibody raised against the C-terminal 59 amino acid residues of rat NK1 receptor (Nakaya et al., 1994).

The guinea pig polyclonal antibody against the NK1 receptor (Biotrend, Cologne, Germany; Cat. no. NA4200) was also raised against the last 23 amino acids (residues 385–407) of the C-terminal domain of the rat sequence. This NK1 antiserum showed an identical labeling pattern as the rabbit one in paraformaldehyde-fixed brain sections.

The rabbit polyclonal anti-parvalbumin antibody (Swant; Cat. no. PV-28, Lot. 5–5) labels a number of brain areas and neurons in control rats and mice. In the cerebellar cortex, Purkinje cells show a particularly prominent staining. This labeling was clearly abolished in PV knockout mice (Caillard et al., 2000).

The mouse monoclonal anti-parvalbumin antibody (Swant; Cat. no. 235, Lot. 10–11) specifically recognized a spot of 12 kDa on a two-dimensional blot of rat cerebellar protein extracts, which is identical to purified parvalbumin. Immunoreactivity in mouse brain sections with this antibody was identical to that reported in previous studies (Celio, 1990), but did not stain the brain of PV knockout mice (manufacturer's datasheets).

The guinea pig polyclonal anti-parvalbumin antibody (Synaptic Systems, Göttingen, Germany; Cat. no. 195004, Lot. 195004/1) was raised against the recombinant full-length rat parvalbumin. All three anti-PV antibodies used here produced identical labeling patterns in the amygdala and hippocampus.

The guinea pig anti-vesicular glutamate transporter (VGluT) 1 antiserum (Chemicon; Cat. no. AB5905, Lot. 23050127) was raised against a synthetic peptide corresponding to residues 541–560 of the rat VGluT1 protein. On Western blot it revealed a single band of 60 kDa (manufacturer's technical information). The pattern of immunohistochemical labeling obtained with this antiserum in rodent brain tissue was identical to that obtained with other rabbit anti-VGluT1 antibodies (Kaneko and Fujiyama, 2002).

The guinea pig anti-VGluT2 antiserum (Chemicon; Cat. no. AB5907, Lot. 23041014) was raised against a synthetic peptide corresponding to residues 565–582 of the rat VGluT2 protein.

Preabsorption of this antiserum with the immunogen synthetic peptide eliminated the immunostaining in tissue sections from rat brain (manufacturer's technical information). The pattern of rodent brain staining was identical to that obtained by Fremeau and coworkers (2001).

The guinea pig anti-VGluT3 antiserum (Chemicon; Cat. no. AB5421, Lot. 23050673) was raised against a synthetic peptide (AFEGEEPLSYQNEEDFSETS) corresponding to part of the rat VGluT3 protein. This antibody to VGluT3 stains brain sections in patterns corresponding to those described from *in situ* hybridization with probes to VGluT3 mRNA. This staining pattern also coincides with the described distribution of immunoreactivity obtained with other VGluT3 antisera (Fremeau et al., 2002). According to the manufacturer, preabsorption of the antiserum with the immunogen peptide eliminates all immunostaining on tissue sections from rat central nervous system.

To control for possible cross-reactivity between IgGs in double and triple immunolabeling experiments, some sections were processed through the same immunocytochemical sequence except that only one primary antibody was applied, but the full complement of secondary antibodies was maintained. In addition, many of the secondary antibodies utilized were highly pre-adsorbed to the IgGs of numerous species. All these control reactions resulted in a lack of labeling of the species-unrelated secondary antibodies, confirming the specificity of the immunosignals.

Sampling procedures

All sections of the LA and BA analyzed were taken between the rostro-caudal levels: bregma −2.30 to −3.30 mm (Paxinos and Watson, 1998). For double and triple immunofluorescence analysis, each neuron expressing a specific marker was analyzed with a 40× objective lens (NA 0.17) and an image for each relevant filter set was taken without modifying the focal plane.

For electron microscopy experiments, NK1-immunopositive profiles (dendrites or spines) were selected only if they were receiving at least one clearly identifiable synapse. The selected profiles were chosen randomly by analyzing the re-embedded specimens. At least three serial sections were analyzed for each synapse on NK1-LI profiles. Sections from three rats were used for these experiments and ultrathin sections from at least two blocks per animal were analyzed.

Statistical analysis

Power analysis was used to establish the sample size of synapses received by NK1/PV-LI profiles required to confidently conclude (α=0.05) whether a significant difference exists between this subgroup and the general population of NK1-LI neurons. We used the free software Piface by R.V Lenth, version 1.72, setting the power to 0.90; the actual value to 15% and the null value to 5%.

To estimate whether the frequency of asymmetric or symmetric synapses differed among the PV-LI, NK1/PV-LI, and the overall NK1-LI profiles, data were analyzed with the chi-square test using the GraphPad Prism software (version 5.0c; GraphPad Software Inc., La Jolla, CA, USA).

RESULTS

Immunoreactivity for NK1 receptors in the rat LA and BA

In the rat BLA, NK1-LI obtained with both rabbit and guinea pig antibodies was associated to the somatodendritic domain of a few discrete neurons (Fig. 1A). At light microscopy level, the distribution and morphology of NK1-immunopositive neurons were identical to previous studies

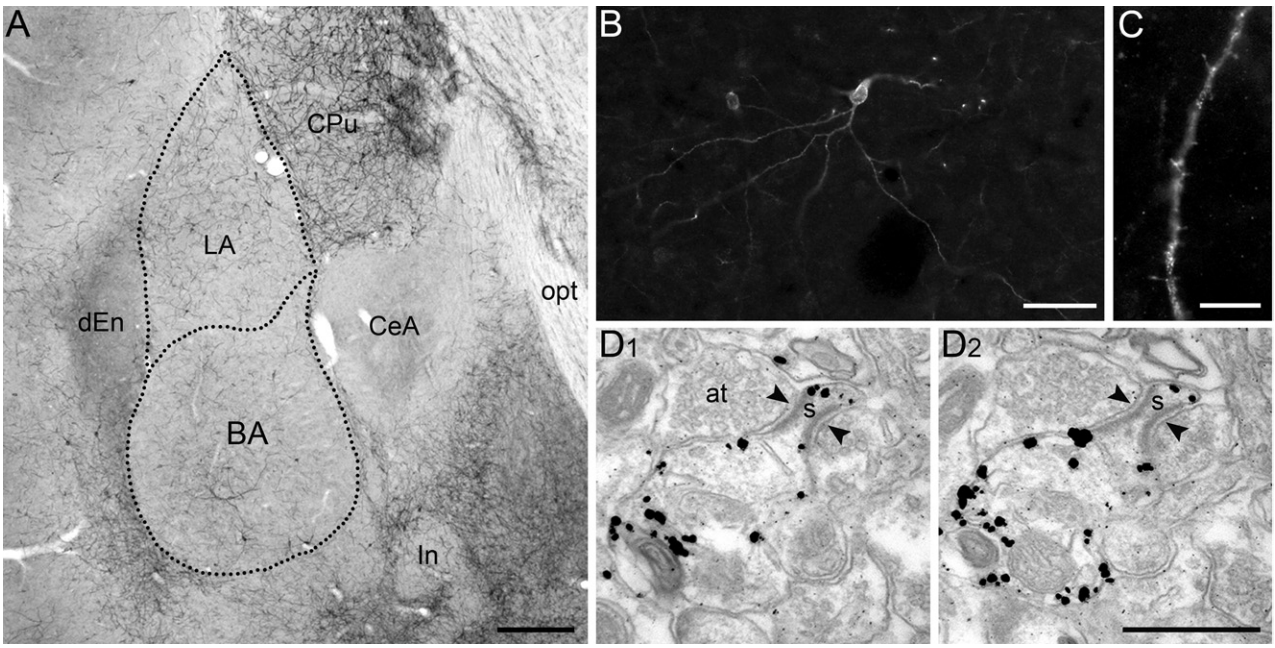

Fig. 1. Photomicrographs of NK1 receptor immunoreactivity in the rat amygdala. (A) NK1 receptor-LI in a coronal section of the amygdala at a mid rostro-caudal level. (B) High power micrograph showing an NK1 receptor-expressing neuron possessing a large dendritic arborization. (C) High power micrograph showing the portion of a dendrite containing sparse spines. (D1, D2) Electron micrographs of two consecutive sections showing a crest-like synapse on an NK1 immunopositive dendrite. Immunoreactivity for NK1 receptor is demonstrated by silver-intensified immunogold reaction. The crest-like spine receives two opposing asymmetrical synapses from unlabeled axon terminals (arrows). Abbreviations: at, axon terminal; BA, basal nucleus; CeA, central nucleus; CPu, striatum; dEn, dorsal endopiriform nucleus; In, main nucleus of the intercalated cell masses; LA, lateral nucleus; opt, optic tract; s, spine. Scale bars: A=500 μm; B=50 μm; C=10 μm; D=500 nm.

(Levita et al., 2003; Nakaya et al., 1994; Singewald et al., 2008). Neurons showing NK1-LI were large and multipolar, although some showed a bipolar shape. They exhibited a large dendritic arborization covering a substantial portion of the respective nucleus (Fig. 1B) with the dendritic branches apparently randomly oriented. In most cases the dendritic length and width appeared to be proportional to the size of the soma. Close immunofluorescence and electron microscopic examinations showed that some NK1-immunoreactive dendrites possessed few spines (Fig. 1C), whereas others appeared to be mostly aspinous. Labeled spines were postsynaptic to axon terminals that formed asymmetric (type I) synapses. Occasionally, we observed crest-like spines originating from small dendrites immunolabeled for NK1 on which two presynaptic terminals formed asymmetric contacts (Fig. 1D).

Expression of calcium binding proteins in NK1-immunoreactive neurons in the rat LA

Double immunofluorescence microscopy experiments were carried out to evaluate the co-distribution between NK1- and CBP-LI in neurons of the rat LA. We also extended our analysis to the BA in order to determine whether the pattern

Table 2. Coexistence between NK1 and Calcium binding proteins in neurons of the BLA

Nucleus	Rat	Cells NK1 positive only (n)	Cells CB positive only (n)	Double labeled cells (n)	Double labeled cells as % of NK1 positive cells	Double labeled cells as % of CB positive cells
Number of NK1-immunopositive, CB-immunopositive, and double-labeled cells						
LA	#1	18	237	10	35.7	5.5
	#2	20	204	10	33.3	4.7
	#3	33	152	13	28.3	7.9
	Total	71	593	33		
	Mean±SEM	23.7±4.7	197.7±24.7	11±1.0	32.4±2.2	6.0±1.0
BA	#1	12	640	47	79.7	6.8
	#2	14	469	27	65.9	5.4
	#3	14	397	35	71.4	8.0
	Total	40	1506	109		
	Mean±SEM	13.3±0.7	502.0±72.1	36.3±5.8	72.3±4.0	6.7±0.8
Nucleus	Rat	Cells NK1 positive only (n)	Cells PV positive only (n)	Double labeled cells (n)	Double labeled cells as % of NK1 positive cells	Double labeled cells as % of PV positive cells
Number of NK1-immunopositive, PV-immunopositive, and double-labeled cells						
LA	#1	31	118	27	46.6	18.6
	#2	91	235	48	34.5	17
	#3	49	190	23	31.9	10.8
	#4	36	153	26	41.9	14.5
	Total	207	696	124		
	Mean±SEM	51.7±13.6	174±25.1	31±5.7	38.7±3.4	15.2±1.7
BA	#1	110	614	0	—	—
	#2	58	691	0	—	—
	#3	61	512	0	—	—
	Total	229	1817	0	—	—
	Mean±SEM	76.3±16.9	605.7±51.8	—		
Nucleus	Rat	Cells NK1 positive only (n)	Cells CR positive only (n)	Double labeled cells (n)	Double labeled cells as % of NK1 positive cells	Double labeled cells as % of CR positive cells
Number of NK1-immunopositive, CR-immunopositive, and double-labeled cells						
LA	#1	36	87	0	—	—
	#2	18	109	0	—	—
	#3	77	157	0	—	—
	Total	131	353	0	—	—
	Mean±SEM	43.7±17.5	117.7±20.7	—		
BA	#1	41	193	0	0	0
	#2	19	155	1	5	0.6
	#3	43	184	2	4.4	1.1
	Total	103	532	3		
	Mean±SEM	34.3±7.7	177.3±11.5	1±0.6	3.1±1.6	0.6±0.3

Data were obtained from three to five sections/animal.
BA, basal nucleus; CB, calbindin; CR, calretinin; LA, lateral nucleus; NK1, neurokinin 1 receptor; PV, parvalbumin.

of co-expression in the two nuclei was similar and to check whether the extent of co-localization obtained under our experimental conditions was comparable with previous studies (Levita et al., 2003; Truitt et al., 2009). To precisely establish the boundaries between LA and BA, in some of the initial experiments we have performed triple immunofluorescence reactions combining antibodies for the VGluT3, NK1, and PV (data not shown), as VGluT3-LI is largely restricted to cholinergic terminals projecting to the BA (Nickerson Poulin et al., 2006).

Analysis of the neuronal co-distribution of NK1- and CB-LI in the LA revealed that approximately 30% of NK1-immunopositive neurons also exhibited CB-LI (Table 2, Fig. 2B). In the BA, we observed the presence of a larger proportion (72% of NK1-LI neurons analyzed) of double-labeled neurons (Table 2, Fig. 3A). Double-labeled neurons corresponded to ~6% of all CB-LI neurons in the LA and ~7% in the BA. Next, we carried out double immunofluorescence experiments followed by an assessment of the extent of PV and NK1 co-expressing neurons. In the LA, approximately 38% of NK1-immunopositive neurons also contained PV-LI (Table 2, Fig. 2D). Conversely, none of the NK1-immunolabeled neurons in the BA (0 out of 229 neurons analyzed) displayed PV-LI (Table 2, Fig. 3C), in line with what was previously reported by Levita et al. (2003). Coexistence of CR- with NK1-LI in BLA neurons was also investigated. Estimation of neurons of the LA containing NK1- and CR-LI showed no coexistence (0 out of 131; Fig. 2F), whereas in the BA ~3% of the neurons displaying NK1-LI also contained CR-LI (Table 2, Fig. 3E), that is, ~0.5% of BA CR-containing neurons.

Because in cortical areas, including LA, various amounts of coexistence between PV and CB have been detected (Gonchar and Burkhalter, 1997; Kubota and Jones, 1993; McDonald and Betette, 2001), triple immunofluorescence experiments were carried out to determine the relative degree of neurons immunoreactive for NK1-LI and containing both PV- and CB-LI. In the triple immuno-

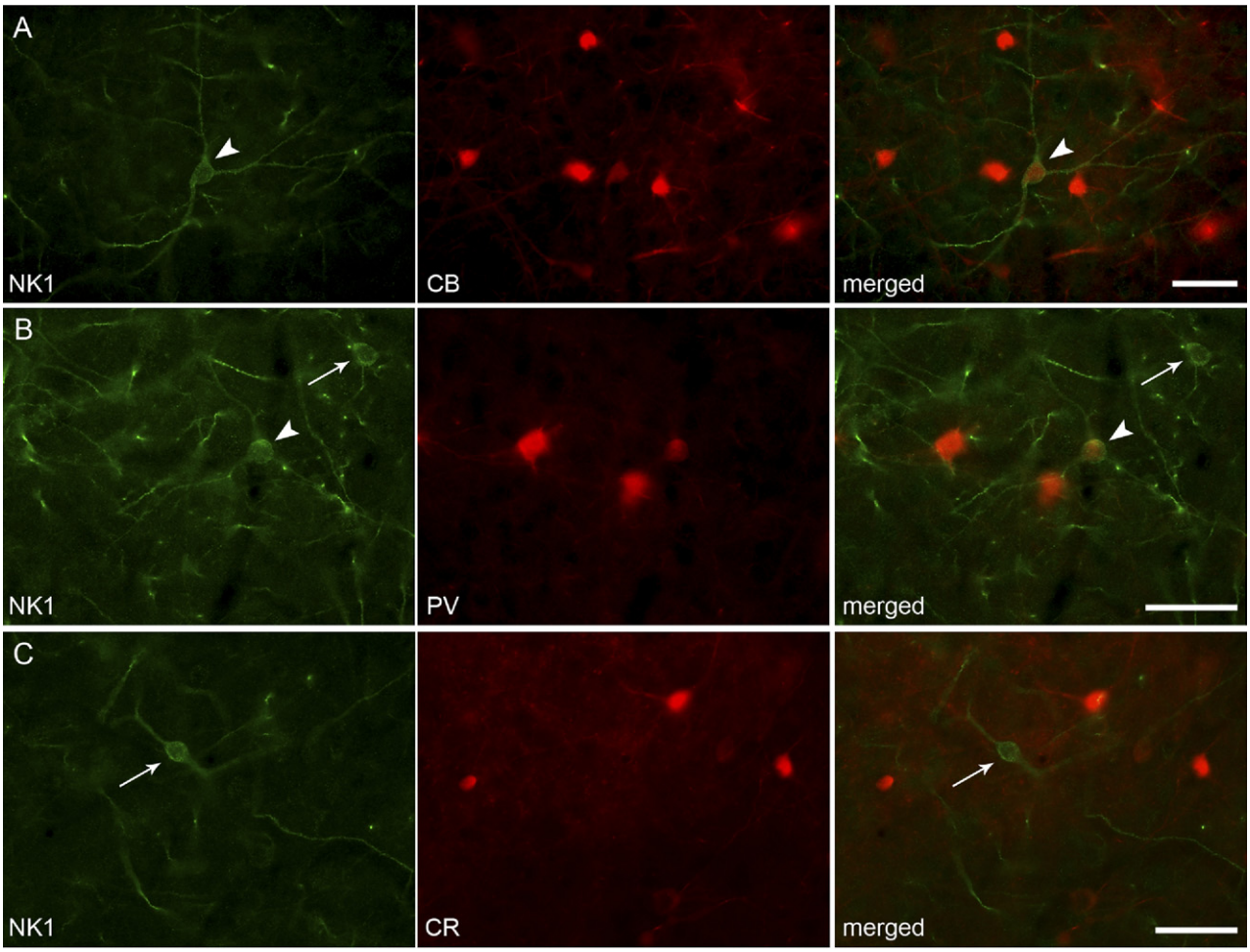

Fig. 2. Co-localization between NK1 receptor and calcium binding proteins in the rat lateral nucleus of the amygdala. Images from double immunofluorescence experiments were taken for each relevant filter set without modifying the focal plane. The column on the left shows NK1-LI neurons (shown in green), the middle column illustrate neurons immunolabeled for different calcium binding proteins (shown in red), whereas the column on the right displays the superimposed images (merged). These panels show representative examples of LA neurons exhibiting co-expression (indicated by arrowheads) between NK1 receptors and (A) calbindin (CB) or (B) parvalbumin (PV). (C) On the other hand, NK1- and calretinin (CR)-LI were not found to co-localize in neurons of the LA. Arrows indicate neurons immunolabeled for the NK1 receptor only. Scale bars: 50 μm. For interpretation of the references to color in this figure legend, the reader is referred to the Web version of this article.

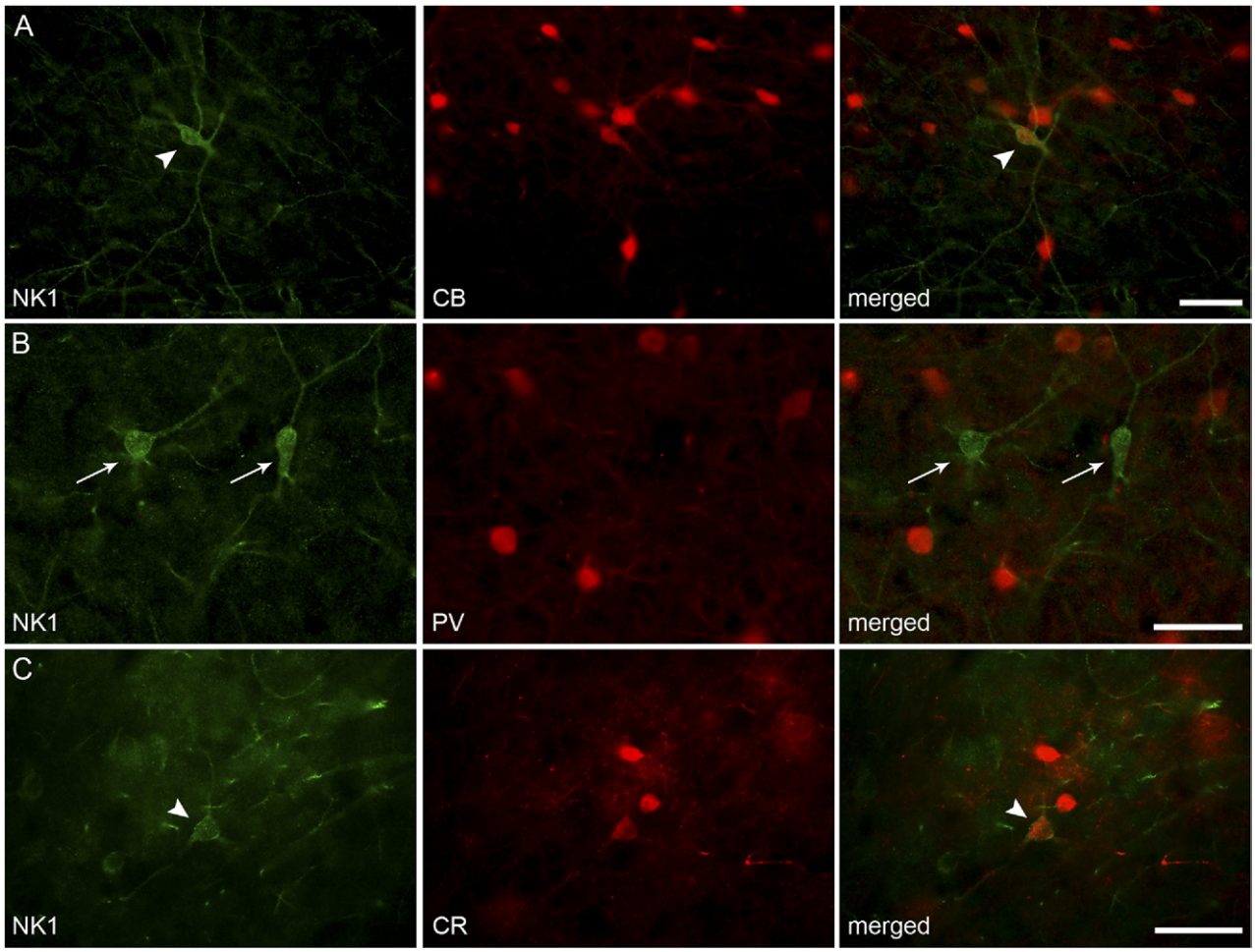

Fig. 3. Co-localization between NK1 receptor and calcium binding proteins in the rat basal nucleus of the amygdala. Images from double immunofluorescence experiments were taken for each relevant filter set without modifying the focal plane. The column on the left shows NK1-LI neurons (shown in green), the middle column illustrate neurons immunolabeled for different calcium binding proteins (shown in red), whereas the column on the right displays the superimposed images (merged). (A) Representative example of BA neurons exhibiting co-expression (indicated by arrowheads) between NK1 receptors and calbindin (CB). (B) In the basal nucleus, immunolabeling for NK1 and parvalbumin (PV) is present in non-overlapping populations of neurons. (C) Although infrequent, co-expression of NK1- and calretinin (CR)-LI was detected in a few BA neurons (indicated by the arrowhead). Arrows indicate neurons immunolabeled for NK1 receptor only. Scale bars: 50 μm. For interpretation of the references to color in this figure legend, the reader is referred to the Web version of this article.

labeling tests for NK1, PV, and CB, we found that ~5% of NK1-positive neurons in the LA were also immunoreactive for both PV and CB (Table 3, Fig. 4). Our study also indicates that CB- and/or PV-LI co-localize with ~60% of NK1-immunopositive neurons in the LA, leaving ~40% of these neurons not associated with any CBP.

In the LA, expression of NK1 receptors appears restricted to GABAergic interneurons

Although previous studies suggested that in the amygdala, neurons expressing CBPs are GABAergic interneurons (Kemppainen and Pitkänen (2000), some pyramidal-like

Table 3. Co-localization between NK1, parvalbumin, and calbindin in neurons of the LA

Nucleus	Rat	Cells NK1 positive only (n)	Double labeled NK1/PV positive cells (n)	Double labeled NK1/CB positive cells (n)	Triple labeled NK1/PV/CB positive cells (n)	NK1/PV double labeled cells as % of NK1 positive cells	NK1/CB double labeled cells as % of NK1 positive cells	Triple labeled cells as % of NK1 positive cells
LA	#1	25	20	12	1	34.4	20.6	1.7
	#2	21	14	15	4	25.9	27.7	7.4
	#3	25	25	15	3	36.7	22.0	4.4
Total	71	59	42	8				
Mean±SEM	23.7±1.3	19.7±3.2	14.0±1.0	2.7±0.9	32.3±3.3	23.4±2.2	4.5±1.7	

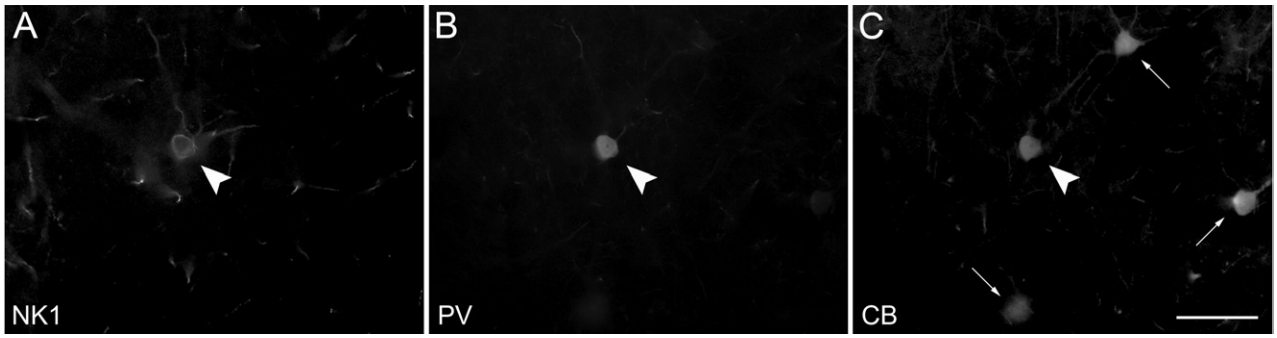

Fig. 4. Triple-immunofluorescence staining for NK1 receptor, PV, and CB in the lateral nucleus of the amygdala. (A) Micrograph showing a neuron immunoreactive for NK1 (arrowhead). (B) The same neuron shows also immunoreactivity for PV. (C) Likewise, CB-LI could be detected in the very same neuron. The arrowhead indicates the same neuron immunopositive for NK1, PV, and CB. Arrows indicate neurons immunoreactive for CB only. Scale bar: 50 μm.

neurons in the BLA were also shown to exhibit low levels of CB- and CR-LI (McDonald, 1994, 1997; McDonald and Mascagni, 2001). In order to establish whether NK1 receptor-expressing neuronal populations in LA correspond to only GABAergic interneurons or both interneurons (e.g. the PV-positive subgroup) and pyramidal-like neurons, an additional set of experiments was carried out to examine the co-expression of NK1 with GAD67 or CaMKIIα. Only a partial co-expression was observed between NK1- and GAD67-LI. In particular, neurons intensely labeled for NK1 did not display detectable GAD67-LI, whereas in weakly or moderately labeled neurons a clear co-expression with GAD67 could be observed (Fig. 5A). In most forebrain regions including the amygdala, CaMKIIα was found exclusively in principle neurons and not in interneurons (Mahanty and Sah, 1998; McDonald et al., 2002; Muller et al., 2006). In double immunofluorescence microscopy experiments with antisera for NK1 and CaMKIIα, we found that NK1-immunopositive neurons were devoid of CaMKIIα-LI (Fig. 5B, C). In order to exclude that, NK1-immunopositive neurons may restrict the expression of CaMKIIα to their dendrites only, we extended our analysis also at the electron microscopy level. CaMKIIα-LI was revealed with silver-intensified immunogold particles, whereas NK1-LI was demonstrated by peroxidase reaction. In NK1 immunolabeled dendrites no CaMKIIα-LI could be detected although immunometal particles were observed in many nearby structures such as axon terminals, spines, and dendritic shafts unlabeled for NK1 and probably belonging to pyramidal-like cells (Fig. 5D). These results provide additional evidence that in the LA NK1 receptors might be expressed solely by interneurons.

NK1 immunoreactive neurons in the LA receive a different degree of VGluT1- or VGluT2-containing glutamatergic inputs

The LA amygdala receives a number of cortical and subcortical glutamatergic inputs (Pitkänen, 2000), which can be at least in part discriminated based on their content of VGluTs, namely VGluT1 and VGluT2 (Fremeau et al., 2004). VGluT1 and VGluT2 show a complementary and mainly reciprocal distribution in the central nervous system. VGluT1 predominates in pyramidal projecting neurons of the neocortex and hippocampus, whereas thalamic, hypothalamic, and parabrachial projection neurons mostly contain VGluT2 at their axonal terminals (Barroso-Chinea et al., 2007; Fremeau et al., 2004; Kaneko and Fujiyama, 2002). Pyramidal-like neurons of the BLA also possess VGluT1; hence, intrinsic afferents in the amygdala arising from these neurons, including local collaterals, contain VGluT1. Therefore, VGluT proteins can be used as reliable markers for defined inputs.

In order to investigate the frequency of VGluT1- and VGluT2-containing inputs onto NK1-expressing neurons in the LA, we carried out double immuno-pre-embedding electron microscopy experiments visualizing VGluT1- or VGluT2-LI by silver-intensified immuno-gold reaction and NK1-LI with immunoperoxidase reaction. Being an enzyme-based reaction, the immunoperoxidase is more sensitive than the immunogold reaction. Therefore, it was used for the visualization of the receptor, which has lower expression levels. Although NK1 receptors are integral membrane proteins and mostly localized on the plasma membrane (Fig. 1D), the NK1-associated peroxidase reaction end product was often observed filling the entire dendrite and/or soma because of its intracellular diffusion. Immunometal particles detecting VGluT1 or VGluT2 were observed only in axon terminals forming asymmetrical synapses on dendrites and spines (Figs. 6 and 7). Each synapse was analyzed in serial ultrathin sections, and in order to define an axon terminal as immunopositive for VGluT1 or VGluT2, clear labeling had to be detectable in at least three sections. To estimate the frequency of synapses made by axon terminals with VGluT1-LI on NK1-immunopositive profiles (dendrites or spines), we have analyzed 92 of such profiles (obtained from three rats), which received on the whole 123 asymmetric (1.33 synapses/profile) and 10 symmetric synapses (0.11 synapses/profile) (Table 4, Fig. 6). Out of these 123 asymmetric synapses, 67 contained VGluT1 immunolabeling in the presynaptic terminal, hence accounting for 54.0$\pm$2.1% of all asymmetric synapses received by NK1-immunoreactive profiles (Table 4). Similarly, to estimate the frequency of

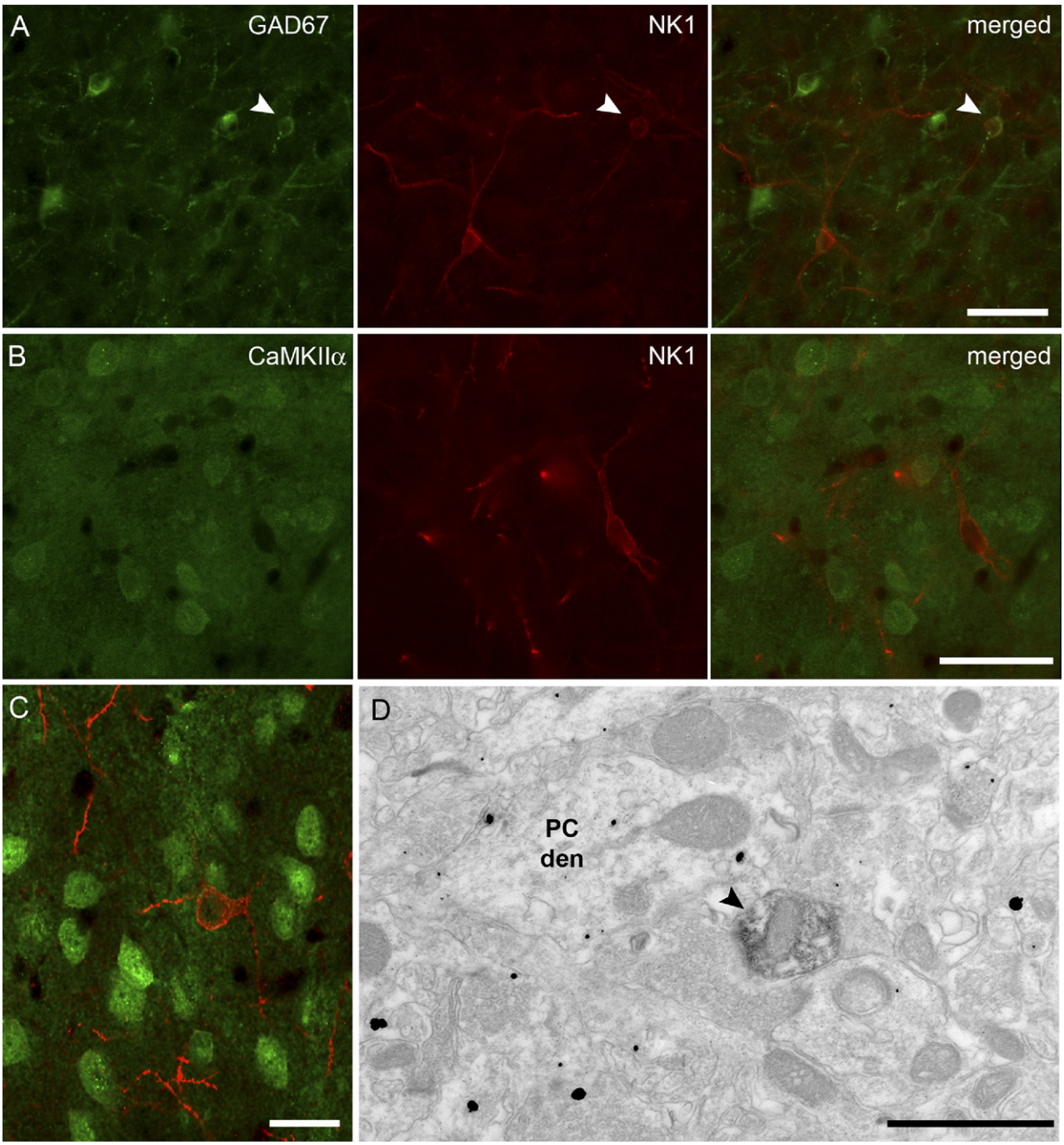

Fig. 5. Neurons expressing NK1 in the lateral nucleus of the amygdala show a partial coexistence with GAD67 but lack CaMKIIα-LI. (A) Micrographs showing the localization of GAD67- (in green) and NK1-LI (in red) in LA. A neuron moderately stained for NK1 co-expresses also GAD67 (indicated by the arrowhead), whereas a strongly labeled neuron does show detectable levels of GAD67-LI. (B) Epifluorescence micrographs taken at the very same focal plane for CaMKIIα, a marker for pyramidal-like neurons, and NK1. Neurons immunoreactive for CaMKIIα (in green) do not display NK1-LI (in red); the blank outline of an NK1 labeled soma can be clearly observed with the Cy2/Alexa488 filter block, which allows the detection of CaMKIIα-LI. (C) Also using confocal fluorescence microscopy to make sure only one focal plane was analyzed, we observed a complete segregation of the immunolabelings for NK1 (in red) and CaMKIIα (in green). (D) Electron micrograph showing a complete segregation between NK1- (peroxidase) and CaMKIIα-LI (immunogold-silver) in dendrites of LA neurons. A dendrite filled with peroxidase end product and revealing NK1 receptor-LI (indicated by the arrowhead) is devoid of immunometal particles visualizing CaMKIIα-LI. Conversely immunometal particles for CaMKIIα can be clearly observed in a nearby dendrite of a pyramidal-like neuron (PC den). Scale bar: A, B=50 μm; C=20 μm; D=1 μm. For interpretation of the references to color in this figure legend, the reader is referred to the Web version of this article.

synapses made by axon terminals with VGluT2-LI, we have analyzed 100 NK1-immunopositive profiles, which received on the whole 126 asymmetric synapses (1.26 synapses/profile) and 13 symmetric synapses (0.13 syn-

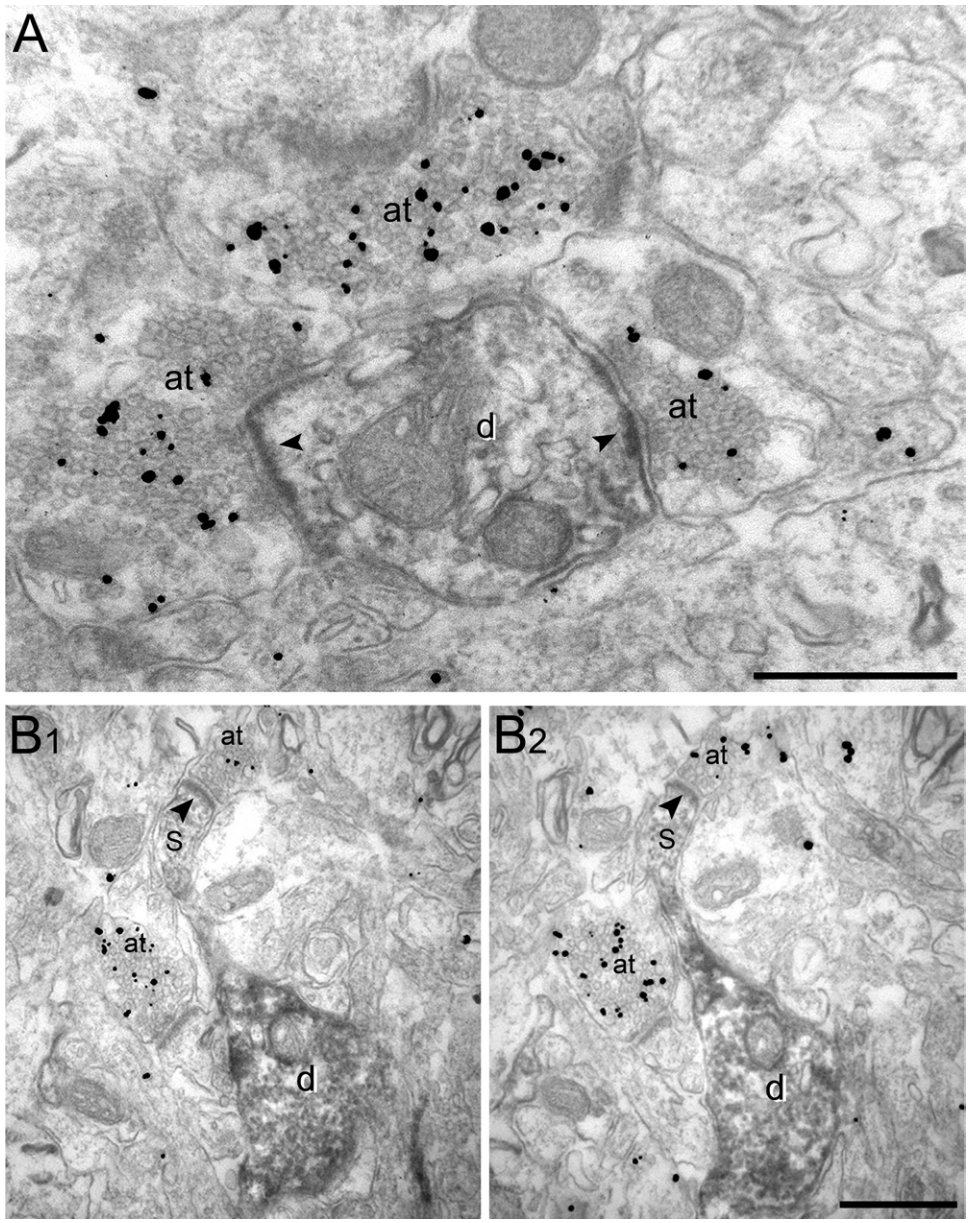

Fig. 6. NK1 immunopositive neurons in the lateral nucleus of the amygdala are innervated by VGluT1-immunolabeled axon terminals. (A) Electron micrograph of two asymmetric synapses (arrowheads) made by axon terminals immunoreactive for VGluT1 (immunogold/silver) onto a dendritic shaft immunoreactive for NK1 (peroxidase). (B1, B2) Electron micrographs of consecutive ultrathin sections of a dendrite labeled for NK1 (peroxidase) emitting a small drumstick spine that receives an asymmetric synapse (arrowhead) from an axon terminal immunoreactive for VGluT1 (immunogold/silver). Abbreviations: d, labeled dendrite; at, axon terminal; s, spine. Scale bars: 500 nm.

apses/profile) (Table 5, Fig. 7). Out of these 126 asymmetric synapses, 23 contained VGluT2-LI in the presynaptic element, hence accounting for 18.3±3.9% of all asymmetric synapses received by NK1-immunolabeled profiles (Table 5).

VGluT2-containing inputs could not be detected at neurons expressing NK1 and PV

Next, we have analyzed whether in the LA the subgroup of neurons co-expressing NK1- and PV-LI receives the same degree of thalamic/hypothalamic or parabrachial innervation as the whole class of NK1-immunopositive cells. To this aim we have carried out triple immuno-pre-embedding electron microscopy experiments detecting at the same time NK1-, PV-, and VGluT2-LI. PV-LI was demonstrated by immunoperoxidase reaction, whereas both VGluT2- and NK1-LI were demonstrated by silver intensified immunogold particles, as labeling for VGluT2 is restricted to presynaptic terminals and NK1-LI could be detected predominantly on postsynaptic elements in the LA. Only very few axon terminals (<0.5%) were observed to contain NK1-LI and these always formed symmetric synapses.

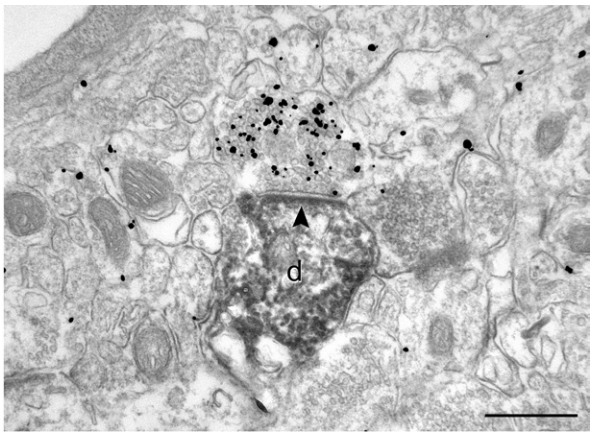

Fig. 7. NK1 immunopositive neurons in the lateral nucleus of the amygdala are also innervated by VGluT2-immunolabeled axon terminals. Electron micrograph of an asymmetric synapse (arrowhead) on a dendritic shaft immunoreactive for NK1 (peroxidase) formed by a presynaptic bouton immunoreactive for VGluT2 (immunogold/silver). Abbreviation: d, labeled dendrite. Scale bars: 500 nm.

Power analysis was used to establish in advance the sample size (≥79) of synapses required to confidently conclude (α=0.05) whether a significant difference might exist between the overall population of NK1-immunoreactive profiles (dendrites/spines) and those immunolabeled also for PV. We have analyzed 64 profiles (obtained from three rats) displaying both NK1- and PV-LI, which received overall 124 asymmetric synapses. Of these synapses none showed VGluT2-LI associated with presynaptic terminals (Table 6, Fig. 8), although clear VGluT2-LI was always present in axon terminals close to NK1/PV-immunoreactive profiles (Fig. 8). These findings clearly demonstrate that NK1-PV-expressing neurons either do not receive or receive only very few inputs containing VGluT2-LI. Furthermore, these neurons appear to possess a higher density of asymmetric synapses (1.95 synapses/profile; P=0.0275, Mann–Whitney test) when compared with the overall population of LA neurons possessing NK1-LI. We also examined in the same reaction 105 profiles possessing only PV-LI. On these profiles we observed 198 asymmetrical synapses (1.84 synapses/profile), 14 of which showed VGluT2-LI in the presynaptic axon terminal, thus representing 7.1±0.8% of all asymmetric synapses received by PV-immunolabeled profiles (Table 7). When the density of VGluT2-positive synapses was compared between profiles containing NK1- or PV-LI, we found that the latter ones received significantly fewer VGluT2-containing inputs (P=0.004 χ^2).

In a similar experiment, NK1-PV-expressing neurons were indeed contacted by axon terminals containing VGluT1 (data not shown). However, because VGluT1 labeling could not differentiate cortical from intrinsic inputs, quantification of these synapses was not carried out.

Gap junctions connect NK1-immunopositive dendrites in the LA

Besides chemical synapses, we found that neurons displaying NK1-LI were also connected through gap junctions in each of the three brains analyzed. Despite the presence of peroxidase immunoreactivity, which was used to detect NK1 receptors, we could reveal the typical ultrastructural features of gap junctions, such as the characteristic convergence of the plasma membranes of two labeled adjacent dendrites (Fig. 9A). A few gap junctions appeared to be bordered by desmosome-like junctions characterized by electrondense undercoatings at the inner leaflets of the junctional membranes (Fig. 9A).

PV positive terminals innervate NK1/PV-immunoreactive dendrites in the LA

Labeling for parvalbumin in the LA was detected in somata, dendrites as well as axon terminals. Axon terminals with PV-LI contained flattened vesicles and formed symmetrical synapses primarily onto the axon initial segment, dendrites, and somata of unlabeled neurons, but also on dendrites and somata of PV immunopositive interneurons, in accordance with previous studies (Muller et al., 2005). We found one NK1 and PV immunolabeled dendrite that received a symmetric synapse from a large PV-containing bouton (Fig. 9B). Despite the anecdotal character of this finding, it suggests that similar to other PV interneurons (Muller et al., 2005) also NK1-PV neurons are innervated either by GABAergic basal forebrain inputs (Mascagni and McDonald, 2009) or other LA interneurons expressing PV.

DISCUSSION

This work contains several key findings. First of all, our work indicates that the expression of NK1 receptors in the LA is limited to interneurons. We then show that the pattern and extent of co-localization of NK1- and CBP-LI largely differ between LA and BA, hence implying a substantial dissimilarity in both the chemo- and cyto-architecture of

Table 4. Frequency of VGluT1-containing synapses onto dendrites of NK1-expressing interneurons in the LA

Rat	No. of profiles analyzed	No. of asymmetric synapses	No. of asymmetric synapses/profile	No. of symmetric synapses	No. of symmetric synapses/profile	Frequency of VGluT1-LI terminals
#1	31	33	1.06	6	0.19	54.5%
#2	33	54	1.64	3	0.09	57.4%
#3	28	36	1.29	1	0.04	50.0%
Total	92	123		10		
Mean±SEM	30.7±1.4	41±6.6	1.33±0.17	3.3±1.4	0.11±0.04	54.0±2.1%

Table 5. Frequency of VGluT2-containing synapses onto dendrites of NK1-expressing interneurons in the LA

Rat	No. of profiles analyzed	No. of asymmetric synapses	No. of asymmetric synapses/profile	No. of symmetric synapses	No. of symmetric synapses/profile	Frequency of VGluT2-LI terminals
#1	36	45	1.25	4	0.11	11.1%
#2	35	45	1.29	6	0.17	24.4%
#3	29	36	1.24	3	0.10	19.4%
Total	100	126		13		
Mean±SEM	33.3±2.2	42±3.0	1.26±0.01	4.3±0.9	0.13±0.02	18.3±3.9%

these two nuclei. In addition, our study suggests that glutamatergic inputs to NK1-expressing neurons in LA originate for approximately 75% from the neocortex, hippocampus, and/or amygdaloid pyramidal neurons, as revealed by VGluT1 labeling, and for 25% from subcortical areas because they contain VGluT2. Finally, we show that the subgroup of NK1 immunopositive neurons co-expressing PV is either not innervated by axon terminals containing VGluT2-LI or these inputs are so infrequent that they could not be detected under our experimental conditions and sampling procedures. A schematic diagram summarizing these findings is shown in Fig. 10.

NK1-LI neuronal subpopulations in the LA

Our work shows a lack of co-expression between NK1- and CaMKIIα-LI in LA neurons and a partial co-localization between GAD67-, a marker for GABAergic neurons, and NK1-LI. These findings taken together with the observed induction of IPSCs by SP in the BLA (Maubach et al., 2001) strongly suggest that the expression of NK1 receptors is limited to interneurons, at least in rodents. Consistent with this suggestion, the localization of NK1-LI in the neocortex and hippocampus was shown to be mostly associated with non-pyramidal cells (Acsady et al., 1997; Kaneko et al., 1994). On the other hand, the lack of GAD67 expression by some NK1 immunolabeled neurons in the LA would indicate that these neurons are either non-GABAergic or have in their somata GAD67 levels below our detection threshold. In previous studies as well as in our own experience, antibodies to GAD67 and GABA were found to stain axon terminals well but to erratically stain cell bodies (Kemppainen and Pitkänen, 2000; Parrish-Aungst et al., 2007; Tamamaki et al., 2003). This hampers, therefore, a complete detection of GABAergic interneurons and does not rule out a neuron lacking GAD67-LI as a possible interneuron.

The current prevalent view is that BA and LA share a comparable cytoarchitecture including the general morphological and electrophysiological features of their interneurons. Our study reveals a major difference in the neurochemical phenotype of NK1 immunopositive neurons in the LA as compared with the BA. In particular, our work shows that in the LA ~35% of NK1-immunolabeled neurons co-expressed PV-LI, unlike what was observed in the BA in which neurons displaying NK1-LI do not express PV (see also Levita et al., 2003). No coexistence was detected between NK1- and CR-LI in LA and was negligible in the BA. Although our study found that the proportion of NK1 immunopositive cells co-expressing CB in the LA was approximately half of that in the BA, the overall percentage of CB immunoreactive neurons containing NK1-LI in the two nuclei was similar. Our data further demonstrated that approximately 12% of neurons containing NK1- and PV-LI also expressed CB. In cortical areas, axons containing both of these CBPs generally originate form basket cells, thus suggesting that LA interneurons expressing PV, CB, and NK1 might be basket cells (McDonald and Betette, 2001). However, in the neocortex dendrite-targeting interneurons expressing both PV and CB have been described (Blatow et al., 2003) and their presence in the BLA has also been recently suggested (Woodruff and Sah, 2007b). Further studies, for example, combining *in vivo* juxtacellular neurobiotin-filling with immunofluorescence and electron microscopy, will have to clarify the axonal pattern of these interneurons.

Based on the co-expression of CBPs, we identify in the LA four neurochemical phenotypes of NK1 immunopositive neurons: (i) those containing PV, which account for ~30%; (ii) those containing CB and representing ~25%; (iii) those containing both CB and PV that comprise 5%; and (iv) those devoid of detectable CBPs-LI. These latter neurons

Table 6. Frequency of VGluT2-containing synapses onto dendrites of NK1/PV expressing interneurons in the LA

Rat	No. of profiles analyzed	No. of asymmetric synapses	No. of asymmetric synapses/profile	No. of symmetric synapses	No. of symmetric synapses/profile	Frequency of VGluT2-LI terminals
#1	26	53	2.04	3	0.11	0%
#2	22	37	1.68	1	0.04	0%
#3	16	34	2.12	0	0	0%
Total	64	124		4		
Mean±SEM	21.3±2.9	41.3±5.9	1.95±0.13	1.3±0.9	0.05±0.03	—

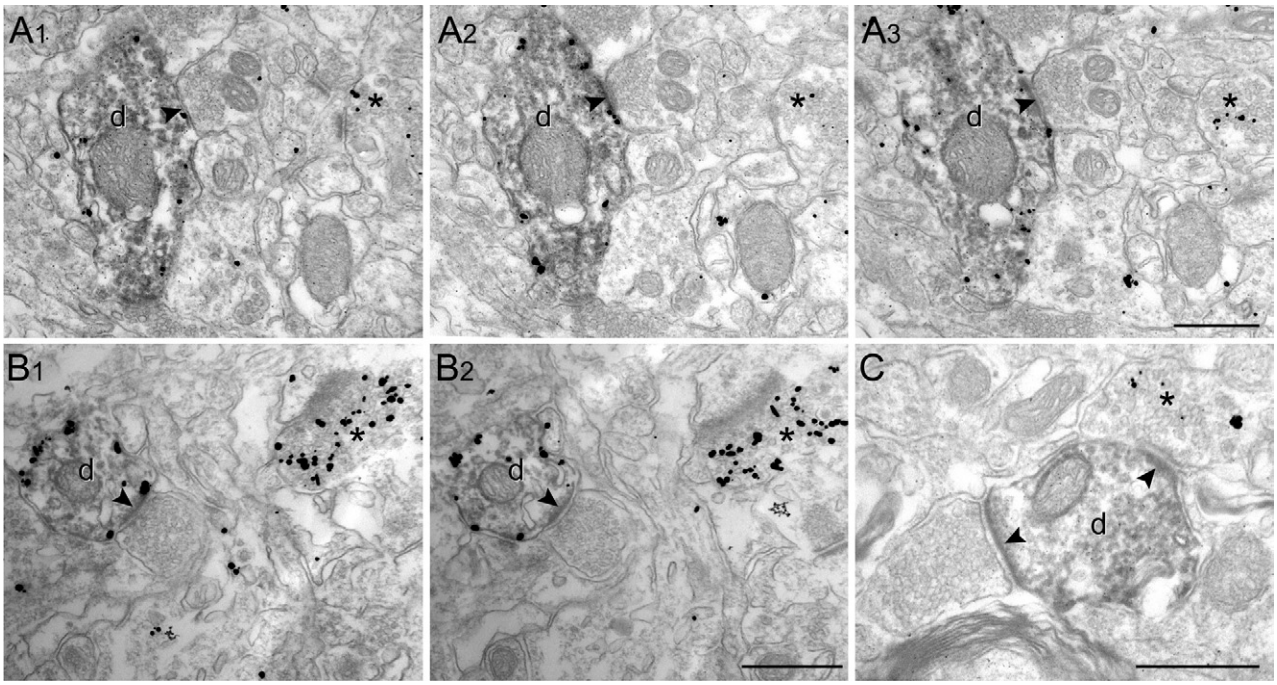

Fig. 8. Lack of detectable innervation by VGluT2-containing axon terminals of NK1 and PV-expressing neurons in the lateral amygdala. (A1–A3) Electron micrographs of consecutive ultrathin sections of a dendritic shaft immunopositive for NK1 (immunogold-silver) and PV (peroxidase) and receiving an unlabeled input forming an asymmetric synapse. (B1, B2) Further example of an NK1 and PV labeled dendrite that receives an asymmetric synapse not containing VGluT2. Noteworthy, VGluT2 immunopositive terminals, also visualized by immunometal particles, can be observed near the labeled dendrites (asterisk). (C) A dendritic shaft immunopositive for PV receives an asymmetric synapse from a VGluT2-labeled terminal (asterisk) as well as from an unlabeled axon terminal. Asymmetric synapses are indicated by arrowheads. Abbreviation: d, labeled dendrite. Scale bar: 500 nm.

may correspond to cholecystokinin-containing interneurons (Truitt et al., 2009).

Inputs to NK1-expressing neurons of the LA

As shown by previous tract-tracing studies, several brain areas give rise to excitatory afferents to the LA (Pitkänen, 2000). These include the thalamus, the ventral hippocampus, various cortical fields, the hypothalamic ventromedial nucleus, and the parabrachial nucleus (Bianchi et al., 1998; Canteras et al., 1994; Kishi et al., 2006; LeDoux et al., 1990; Pitkänen, 2000; Romanski and LeDoux, 1993). In particular, the LA receives abundant auditory sensory inputs both from the thalamus and cortex, and serves as the sensory interface of the amygdala (Doron and Ledoux, 1999; McDonald, 1998). These excitatory inputs innervate both pyramidal-like cells and interneurons (Carlsen and Heimer, 1988; Farb and LeDoux, 1997; LeDoux et al., 1990; Smith et al., 1998; Woodson et al., 2000), but so far the relation between specific afferents and subtypes of inhibitory interneurons of the LA has received little attention. To our knowledge this study is the first to examine quantitatively the contribution of different excitatory inputs onto neurochemically-identified subclasses of LA interneurons. Our findings indicate that at least 72% of all asymmetric synapses received by NK1-immunopositive neurons display either VGluT1- or VGluT2-LI, hence glutamatergic in nature. However, it should be kept in mind that our experimental approach most likely underestimates the number of terminals containing VGluTs, for example, because of incomplete penetration of the antibodies. Besides glutamatergic axon terminals also cholinergic and noradrenergic ones can form asymmetric synapses in the amygdala (Li et al., 2002; Nitecka and Frotscher, 1989). However, the LA receives little cholinergic and moderate

Table 7. Frequency of VGluT2-containing synapses onto dendrites of PV-expressing interneurons of the LA

Rat	No. of profiles analyzed	No. of asymmetric synapses	No. of asymmetric synapses/profile	No. of symmetric synapses	No. of symmetric synapses/profile	Frequency of VGluT2-LI terminals
#1	45	98	2.18	9	0.20	7.1%
#2	29	53	1.83	3	0.10	5.7%
#3	31	47	1.51	2	0.06	8.5%
Total	105	198		14		
Mean±SEM	35±5.0	66±16.1	1.84±0.19	4.7±2.2	0.12±0.04	7.1±0.8%

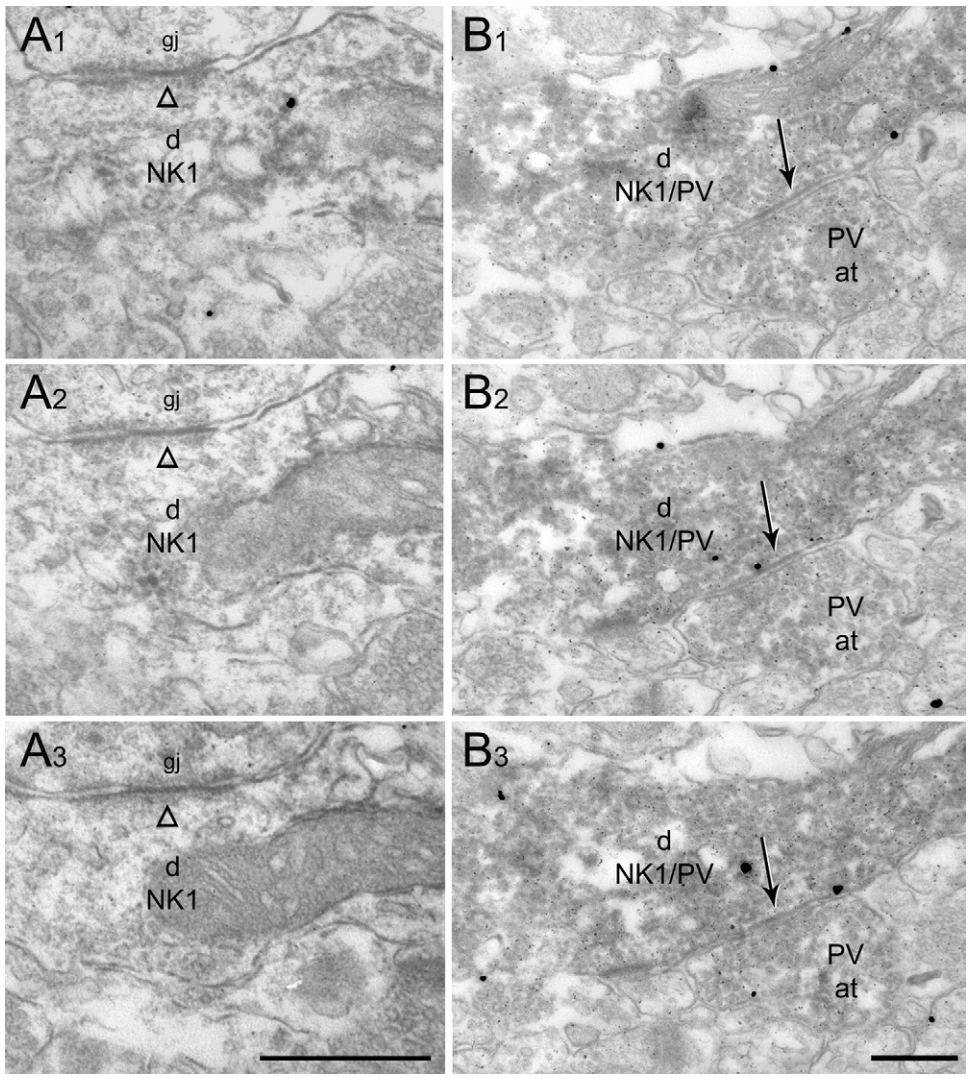

Fig. 9. Dendritic shafts of NK1-expressing interneurons in the lateral amygdala receive symmetric synapses containing PV and are interconnected through gap junctions. (A1–A3) Consecutive electron micrographs of a gap junction (indicated by the empty arrowhead) between two NK1-immunopositive dendrites. (B1–B3). Electron micrographs from consecutive ultrathin sections of an axon terminal displaying PV-LI and forming a symmetrical synapse (indicated by the arrow) with an NK1/PV immunopositive dendritic shaft. PV-LI is demonstrated by peroxidase reaction, whereas NK1-LI is revealed by immunogold-silver reaction. Abbreviations: at PV, axon terminal labeled for PV; d NK1, dendrite labeled for NK1; d NK1/PV, dendrite labeled for both PV and NK1; gj, gap junction. Scale bars: 500 nm.

noradrenergic innervation (Li et al., 2002; Nickerson Poulin et al., 2006) suggesting that the vast majority of asymmetric synapses in the LA are in fact glutamatergic.

Our study suggests that ~25% of glutamatergic inputs to LA NK1-positive neurons originate from thalamic, hypothalamic, or parabrachial inputs, hence a far larger proportion than what was previously observed or proposed for BLA interneurons (Smith et al., 2000; Woodson et al., 2000). One of the main findings of our study is either the lack of or scarce innervation of PV/NK1 neurons by VGluT2-containing axon terminals. This suggests that at least some of the other NK1-expressing neurons devoid of PV receive a denser innervation from diencephalic or brain stem areas than what was estimated for the entire population of NK1-expressing neurons in the LA. These interneurons may thus subserve feedforward inhibition. Previous ultrastructural studies have shown that interneurons displaying PV-LI in the cat BA are primarily innervated from intrinsic pyramidal-like neurons than from cortical inputs (McDonald et al., 2005; Smith et al., 2000). This may also be the case for PV/NK1-positive interneurons in the LA and would imply that this cell class is preferentially involved in the genesis of feedback inhibition. Our data substantiate previous physiological studies showing that LA principal neurons are at first excited and then inhibited by stimulation of the auditory thalamus (Clugnet and LeDoux, 1990; Li et al., 1996). This inhibition may in fact arise from both feedback and feedforward mechanisms involving local inhibitory interneurons (Fig. 10).

Our study shows that at least some NK1-LI neurons in the LA are also coupled through electrical synapses. Because PV-containing interneurons of the BA, as well as of

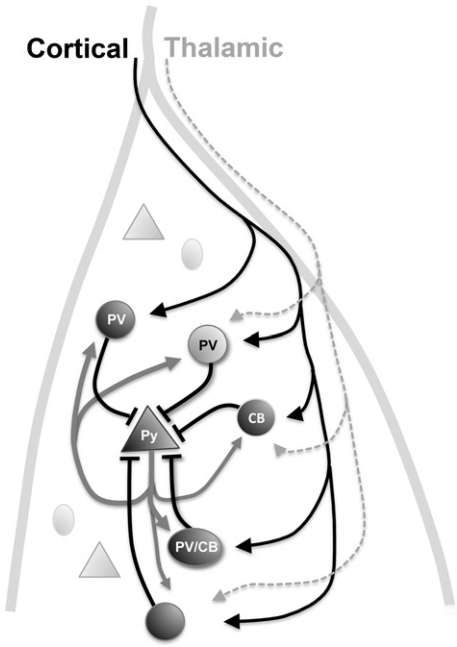

Fig. 10. Schematic diagram of the different neurochemical phenotypes of NK1 receptor-expressing interneuron and of their main glutamatergic afferents within the lateral nucleus of the amygdala. NK1 receptor-expressing interneuron are shown here as round or ovoidal shapes in dark gray. Cortical/hippocampal inputs are shown as black arrows whereas thalamic/hypothalamic/parabrachial afferents, shortened here as thalamic, are exemplified with light gray dashed arrows. Intrinsic afferents from pyramidal neurons (triangle) are shown as dark gray arrows. Parvalbumin (PV) interneurons lacking NK1-LI are also included in light gray. These schematic pathways illustrate the possible participation of these interneurons in feedback or feedforward inhibition.

other cortical regions, are known to be interconnected through gap junctions (Muller et al., 2005), we suggest that the NK1-LI neurons displaying dendro-dendritic gap junctions may belong to the subset of NK1/PV interneurons. This electrical coupling between NK1-expressing neurons may facilitate the degree of synchronization of their activity and participation to the generation of rhythmic oscillations in the LA (Cobb et al., 1995; Woodruff and Sah, 2007a).

In the cat BA, symmetric synapses account for 10–15% of synaptic specializations onto pyramidal-like cells (Narkiewicz et al., 1978) and to less than 10% onto interneurons (Smith et al., 1998). Our study shows that the frequency of symmetrical synapses on NK1-LI neurons in the rat LA is similar (6.4%) to what was previously reported for interneurons in the cat BA. This finding implies that these interneurons are subjected to comparatively less inhibition than pyramidal-like cells.

Functional implications

NK1-expressing neurons in the BLA represent a relatively small proportion (~3%) of the total GABAergic population (Truitt et al., 2009). However, pharmacological and neurotoxic lesion studies have shown that local activation or inhibition/ablation of these interneurons can dramatically influence BLA activity and animal behavior (Boyce et al., 2001; Rupniak et al., 2003; Truitt et al., 2007). Gene-targeted deletion of NK1 as well as toxin-mediated ablation of NK1 receptor-expressing neurons in the amygdala abolished conditioned place preference to morphine, suggesting a role for these interneurons in morphine reward (Gadd et al., 2003; Murtra et al., 2000). Moreover, genetic disruption of NK1-receptor function markedly reduced anxiety-related behaviors in the elevated plus maze, novelty-suppressed feeding, and maternal separation paradigms (Santarelli et al., 2001). Similarly, selective NK1 receptor antagonists elicited antidepressant and anxiolytic effects and inhibited conditioned fear (Boyce et al., 2001; Heldt et al., 2009; Rupniak et al., 2003; Varty et al., 2002). On the other hand, restricted ablation of NK1 receptor-expressing neurons of the BA enhanced fear- and anxiety-like responses (Truitt et al., 2009). Taken together these findings suggest that NK1-containing neurons of the LA and BA participate to distinct intrinsic neural circuits with different if not opposite functions in modulating fear- and anxiety-like responses. Single-unit studies performed in non-anesthetized cats showed that the spontaneous firing rate of projection neurons is generally lower in the LA than in the BA (Gaudreau and Pare, 1996; Pare and Gaudreau, 1996). Thus differences in inhibitory circuits in the two nuclei may account for these differences, and NK1-containing interneurons may contribute to this difference.

Neurons synthesizing SP in the amygdala are located almost exclusively in the central and medial nuclei (Roberts et al., 1982), whereas the BLA contains only sparse axons containing this neuropeptide that are not in direct contact with NK1-expressing neurons (Roberts et al., 1982; Singewald et al., 2008). The activation of NK1 receptors in the BLA may thus result from volume transmission (Agnati et al., 2010), and would consequently enhance the excitability of BLA interneurons contributing in turn to the inhibition of pyramidal-like cells. We can hypothesize that the enhanced release of SP during fear states and stress (Ebner and Singewald, 2006) produces a delayed but pronounced excitation of BLA interneurons bearing NK1 receptors. The sparsely distributed NK1-containing interneurons in the LA may thus have the unique function of synchronizing in stress conditions the firing of pyramidal-like neurons with that of incoming inputs for the integration and binding of emotionally salient stimuli.

CONCLUSIONS

We propose that LA and BA differ in some of the organizational principles of their inhibitory networks. In the LA, interneurons expressing NK1 receptors possess four distinct neurochemical phenotypes, which also appear to differ in terms of glutamatergic afferents. Based on the distinctive innervation of these interneurons, we postulate that they are respectively involved in feedback or feedforward inhibition. The activation of NK1-expressing interneurons would increase inhibition of LA pyramidal-like neurons and synchronize their firing to incoming sensory inputs, probably facilitating generalization of fear and/or anxiety, particularly under stress conditions.

Acknowledgments—We thank H. Hörtnagel, Y. Kasugai and D. Busti (Dept. Pharmacology, Innsbruck Medical University) for reading a previous version of the manuscript. We also gratefully acknowledge M. Offterdinger for helping with the confocal microscope and Gabi Schmid (Dept. Pharmacology, Innsbruck Medical University) for excellent technical support. This work was supported by the Austrian Science Foundation-Fonds zur Förderung der wissenschaftlichen Forschung (FWF), grant No. S10207 to F.F.

REFERENCES

Acsady L, Katona I, Gulyas AI, Shigemoto R, Freund TF (1997) Immunostaining for substance P receptor labels GABAergic cells with distinct termination patterns in the hippocampus. J Comp Neurol 378:320–336.

Agnati LF, Guidolin D, Guescini M, Genedani S, Fuxe K (2010) Understanding wiring and volume transmission. Brain Res Rev 64:137–159.

Barroso-Chinea P, Castle M, Aymerich MS, Pérez-Manso M, Erro E, Tuñon T, Lanciego JL (2007) Expression of the mRNAs encoding for the vesicular glutamate transporters 1 and 2 in the rat thalamus. J Comp Neurol 501:703–715.

Bianchi R, Corsetti G, Rodella L, Tredici G, Gioia M (1998) Supraspinal connections and termination patterns of the parabrachial complex determined by the biocytin anterograde tract-tracing technique in the rat. J Anat 193(Pt 3):417–430.

Blatow M, Rozov A, Katona I, Hormuzdi SG, Meyer AH, Whittington MA, Caputi A, Monyer H (2003) A novel network of multipolar bursting interneurons generates theta frequency oscillations in neocortex. Neuron 38:805–817.

Boyce S, Smith D, Carlson E, Hewson L, Rigby M, O'Donnell R, Harrison T, Rupniak NM (2001) Intra-amygdala injection of the substance P [NK(1) receptor] antagonist L-760735 inhibits neonatal vocalisations in guinea-pigs. Neuropharmacology 41:130–137.

Caillard O, Moreno H, Schwaller B, Llano I, Celio MR, Marty A (2000) Role of the calcium-binding protein parvalbumin in short-term synaptic plasticity. Proc Natl Acad Sci U S A 97:13372–13377.

Canteras NS, Simerly RB, Swanson LW (1994) Organization of projections from the ventromedial nucleus of the hypothalamus: a Phaseolus vulgaris-leucoagglutinin study in the rat. J Comp Neurol 348:41–79.

Carlsen J, Heimer L (1988) The basolateral amygdaloid complex as a cortical-like structure. Brain Res 441:377–380.

Celio MR (1990) Calbindin D-28k and parvalbumin in the rat nervous system. Neuroscience 35:375–475.

Clugnet MC, LeDoux JE (1990) Synaptic plasticity in fear conditioning circuits: induction of LTP in the lateral nucleus of the amygdala by stimulation of the medial geniculate body. J Neurosci 10: 2818–2824.

Cobb SR, Buhl EH, Halasy K, Paulsen O, Somogyi P (1995) Synchronization of neuronal activity in hippocampus by individual GABAergic interneurons. Nature 378:75–78.

Doron NN, Ledoux JE (1999) Organization of projections to the lateral amygdala from auditory and visual areas of the thalamus in the rat. J Comp Neurol 412:383–409.

Ebner K, Singewald N (2006) The role of substance P in stress and anxiety responses. Amino Acids 31:251–272.

Erondu NE, Kennedy MB (1985) Regional distribution of type II Ca^{2+}/calmodulin-dependent protein kinase in rat brain. J Neurosci 5:3270–3277.

Farb CR, LeDoux JE (1997) NMDA and AMPA receptors in the lateral nucleus of the amygdala are postsynaptic to auditory thalamic afferents. Synapse 27:106–121.

Farb CR, Ledoux JE (1999) Afferents from rat temporal cortex synapse on lateral amygdala neurons that express NMDA and AMPA receptors. Synapse 33:218–229.

Ferraguti F, Cobden P, Pollard M, Cope D, Shigemoto R, Watanabe M, Somogyi P (2004) Immunolocalization of metabotropic glutamate receptor 1alpha (mGluR1alpha) in distinct classes of interneuron in the CA1 region of the rat hippocampus. Hippocampus 14:193–215.

Fremeau RT Jr, Burman J, Qureshi T, Tran CH, Proctor J, Johnson J, Zhang H, Sulzer D, Copenhagen DR, Storm-Mathisen J, Reimer RJ, Chaudry FA, Edwards RH (2002) The identification of vesicular glutamate transporter 3 suggests novel modes of signaling by glutamate. Proc Natl Acad Sci U S A 99:14488–14493.

Fremeau RT Jr, Troyer MD, Pahner I, Nygaard GO, Tran CH, Reimer RJ, Bellocchio EE, Fortin D, Storm-Mathisen J, Edwards RH (2001) The expression of vesicular glutamate transporters defines two classes of excitatory synapse. Neuron 31:247–260.

Fremeau RT Jr, Voglmaier S, Seal RP, Edwards RH (2004) VGLUTs define subsets of excitatory neurons and suggest novel roles for glutamate. Trends Neurosci 27:98–103.

Furmark T, Appel L, Michelgård A, Wahlestedt K, Ahs F, Zancan S, Jacobsson E, Flyckt K, Grohp M, Bergström M, Pich EM, Nilsson LG, Bani M, Langström B, Fredrikson M (2005) Cerebral blood flow changes after treatment of social phobia with the neurokinin-1 antagonist GR205171, citalopram, or placebo. Biol Psychiatry 58:132–142.

Gadd CA, Murtra P, De Felipe C, Hunt SP (2003) Neurokinin-1 receptor-expressing neurons in the amygdala modulate morphine reward and anxiety behaviors in the mouse. J Neurosci 23:8271–8280.

Gaudreau H, Pare D (1996) Projection neurons of the lateral amygdaloid nucleus are virtually silent throughout the sleep–waking cycle. J Neurophysiol 75:1301–1305.

Gonchar Y, Burkhalter A (1997) Three distinct families of GABAergic neurons in rat visual cortex. Cereb Cortex 7:347–358.

Heldt SA, Davis M, Ratti E, Corsi M, Trist D, Ressler KJ (2009) Anxiolytic-like effects of the neurokinin 1 receptor antagonist GR-205171 in the elevated plus maze and contextual fear-potentiated startle model of anxiety in gerbils. Behav Pharmacol 20:584–595.

Kaneko T, Fujiyama F (2002) Complementary distribution of vesicular glutamate transporters in the central nervous system. Neurosci Res 42:243–250.

Kaneko T, Shigemoto R, Nakanishi S, Mizuno N (1994) Morphological and chemical characteristics of substance P receptor-immunoreactive neurons in the rat neocortex. Neuroscience 60:199–211.

Kemppainen S, Pitkänen A (2000) Distribution of parvalbumin, calretinin, and calbindin-D(28k) immunoreactivity in the rat amygdaloid complex and colocalization with gamma-aminobutyric acid. J Comp Neurol 426:441–467.

Kishi T, Tsumori T, Yokota S, Yasui Y (2006) Topographical projection from the hippocampal formation to the amygdala: a combined anterograde and retrograde tracing study in the rat. J Comp Neurol 496:349–368.

Kubota Y, Jones EG (1993) Co-localization of two calcium binding proteins in GABA cells of rat piriform cortex. Brain Res 600: 339–344.

LeDoux JE, Farb C, Ruggiero DA (1990) Topographic organization of neurons in the acoustic thalamus that project to the amygdala. J Neurosci 10:1043–1054.

Levita L, Mania I, Rainnie DG (2003) Subtypes of substance P receptor immunoreactive interneurons in the rat basolateral amygdala. Brain Res 981:41–51.

Li R, Nishijo H, Ono T, Ohtani Y, Ohtani O (2002) Synapses on GABAergic neurons in the basolateral nucleus of the rat amygdala: double-labeling immunoelectron microscopy. Synapse 43:42–50.

Li XF, Armony JL, LeDoux JE (1996) GABAA and GABAB receptors differentially regulate synaptic transmission in the auditory thalamo-amygdala pathway: an *in vivo* microiontophoretic study and a model. Synapse 24:115–124.

Mahanty NK, Sah P (1998) Calcium-permeable AMPA receptors mediate long-term potentiation in interneurons in the amygdala. Nature 394:683–687.

Mascagni F, McDonald AJ (2009) Parvalbumin-immunoreactive neurons and GABAergic neurons of the basal forebrain project to the rat basolateral amygdala. Neuroscience 160:805–812.

Mascagni F, Muly EC, Rainnie DG, McDonald AJ (2009) Immunohistochemical characterization of parvalbumin-containing interneurons in the monkey basolateral amygdala. Neuroscience 158: 1541–1550.

Maubach KA, Martin K, Smith DW, Hewson L, Frankshun RA, Harrison T, Seabrook GR (2001) Substance P stimulates inhibitory synaptic transmission in the guinea pig basolateral amygdala *in vitro*. Neuropharmacology 40:806–817.

McDonald AJ (1984) Neuronal organization of the lateral and basolateral amygdaloid nuclei in the rat. J Comp Neurol 222:589–606.

McDonald AJ (1992) Projection neurons of the basolateral amygdala: a correlative Golgi and retrograde tract tracing study. Brain Res Bull 28:179–185.

McDonald AJ (1994) Calretinin immunoreactive neurons in the basolateral amygdala of the rat and monkey. Brain Res 667:238–242.

McDonald AJ (1997) Calbindin-D28k immunoreactivity in the rat amygdala. J Comp Neurol 383:231–244.

McDonald AJ (1998) Cortical pathways to the mammalian amygdala. Prog Neurobiol 55:257–332.

McDonald AJ, Betette RL (2001) Parvalbumin-containing neurons in the rat basolateral amygdala: morphology and co-localization of calbindin-D(28k). Neuroscience 102:413–425.

McDonald AJ, Mascagni F (2001) Colocalization of calcium-binding proteins and GABA in neurons of the rat basolateral amygdala. Neuroscience 105:681–693.

McDonald AJ, Mascagni F, Mania I, Rainnie DG (2005) Evidence for a perisomatic innervation of parvalbumin-containing interneurons by individual pyramidal cells in the basolateral amygdala. Brain Res 1035:32–40.

McDonald AJ, Muller JF, Mascagni F (2002) GABAergic innervation of alpha type II calcium/calmodulin-dependent protein kinase immunoreactive pyramidal neurons in the rat basolateral amygdala. J Comp Neurol 446:199–218.

McLean S (2005) Do substance P and the NK1 receptor have a role in depression and anxiety? Curr Pharm Des 11:1529–1547.

Muller JF, Mascagni F, McDonald AJ (2005) Coupled networks of parvalbumin-immunoreactive interneurons in the rat basolateral amygdala. J Neurosci 25:7366–7376.

Muller JF, Mascagni F, McDonald AJ (2006) Pyramidal cells of the rat basolateral amygdala: synaptology and innervation by parvalbumin-immunoreactive interneurons. J Comp Neurol 494:635–650.

Murtra P, Sheasby AM, Hunt SP, De Felipe C (2000) Rewarding effects of opiates are absent in mice lacking the receptor for substance P. Nature 405:180–183.

Nakaya Y, Kaneko T, Shigemoto R, Nakanishi S, Mizuno N (1994) Immunohistochemical localization of substance P receptor in the central nervous system of the adult rat. J Comp Neurol 347:249–274.

Narkiewicz O, Juraniec J, Wrzołkowa T (1978) The distribution of axon terminals with flattened vesicles in the nuclei of the amygdaloid body of the cat. J Hirnforsch 19:133–143.

Nickerson Poulin A, Guerci A, El Mestikawy S, Semba K (2006) Vesicular glutamate transporter 3 immunoreactivity is present in cholinergic basal forebrain neurons projecting to the basolateral amygdala in rat. J Comp Neurol 498:690–711.

Nitecka L, Frotscher M (1989) Organization and synaptic interconnections of GABAergic and cholinergic elements in the rat amygdaloid nuclei: single- and double-immunolabeling studies. J Comp Neurol 279:470–488.

Pare D, Gaudreau H (1996) Projection cells and interneurons of the lateral and basolateral amygdala: distinct firing patterns and differential relation to theta and delta rhythms in conscious cats. J Neurosci 16:3334–3350.

Parrish-Aungst S, Shipley MT, Erdelyi F, Szabo G, Puche AC (2007) Quantitative analysis of neuronal diversity in the mouse olfactory bulb. J Comp Neurol 501:825–836.

Paxinos G, Watson C (1998) The rat brain in stereotaxic coordinates. San Diego: Academic Press.

Piggins HD, Samuels RE, Coogan AN, Cutler DJ (2001) Distribution of substance P and neurokinin-1 receptor immunoreactivity in the suprachiasmatic nuclei and intergeniculate leaflet of hamster, mouse, and rat. J Comp Neurol 438:50–65.

Pitkänen A (2000) Connectivity of the rat amygdaloid complex. In: The amygdala. A functional analysis, 2nd ed. (Aggleton JP, ed), pp 31–115. Oxford: Oxford University Press.

Roberts GW, Woodhams PL, Polak JM, Crow TJ (1982) Distribution of neuropeptides in the limbic system of the rat: the amygdaloid complex. Neuroscience 7:99–131.

Romanski LM, LeDoux JE (1993) Information cascade from primary auditory cortex to the amygdala: corticocortical and corticoamygdaloid projections of temporal cortex in the rat. Cereb Cortex 3:515–532.

Rupniak NM, Webb JK, Fisher A, Smith D, Boyce S (2003) The substance P (NK1) receptor antagonist L-760735 inhibits fear conditioning in gerbils. Neuropharmacology 44:516–523.

Sah P, Faber ES, Lopez De Armentia M, Power J (2003) The amygdaloid complex: anatomy and physiology. Physiol Rev 83:803–834.

Santarelli L, Gobbi G, Debs PC, Sibille ET, Blier P, Hen R, Heath MJ (2001) Genetic and pharmacological disruption of neurokinin 1 receptor function decreases anxiety-related behaviors and increases serotonergic function. Proc Natl Acad Sci U S A 98:1912–1917.

Singewald N, Chicchi GG, Thurner CC, Tsao KL, Spetea M, Schmidhammer H, Sreepathi HK, Ferraguti F, Singewald GM, Ebner K (2008) Modulation of basal and stress-induced amygdaloid substance P release by the potent and selective NK1 receptor antagonist L-822429. J Neurochem 106:2476–2488.

Smith Y, Paré JF, Paré D (1998) Cat intraamygdaloid inhibitory network: ultrastructural organization of parvalbumin-immunoreactive elements. J Comp Neurol 391:164–179.

Smith Y, Paré JF, Paré D (2000) Differential innervation of parvalbumin-immunoreactive interneurons of the basolateral amygdaloid complex by cortical and intrinsic inputs. J Comp Neurol 416:496–508.

Sorvari H, Soininen H, Paljärvi L, Karkola K, Pitkänen A (1995) Distribution of parvalbumin-immunoreactive cells and fibers in the human amygdaloid complex. J Comp Neurol 360:185–212.

Sosulina L, Graebenitz S, Pape HC (2010) GABAergic interneurons in the mouse lateral amygdala: a classification study. J Neurophysiol 104:617–626.

Sosulina L, Meis S, Seifert G, Steinhäuser C, Pape HC (2006) Classification of projection neurons and interneurons in the rat lateral amygdala based upon cluster analysis. Mol Cell Neurosci 33:57–67.

Spampanato J, Polepalli J, Sah P (2011) Interneurons in the basolateral amygdala. Neuropharmacology 60:765–773.

Sreepathi HK, Ferraguti F (2008) Differential pattern of co-expression between the substance P receptor NK1 and calcium binding proteins in the lateral and basal nuclei of the amygdala. In: Proceedings of the 6th European Forum of European Neuroscience (FENS, ed). Geneva, Switzerland.

Tamamaki N, Yanagawa Y, Tomioka R, Miyazaki J-I, Obata K, Kaneko T (2003) Green fluorescent protein expression and colocalization with calretinin, parvalbumin, and somatostatin in the GAD67-GFP knock-in mouse. J Comp Neurol 467:60–79.

Truitt WA, Johnson PL, Dietrich AD, Fitz SD, Shekhar A (2009) Anxiety-like behavior is modulated by a discrete subpopulation of interneurons in the basolateral amygdala. Neuroscience 160:284–294.

Truitt WA, Sajdyk TJ, Dietrich AD, Oberlin B, McDougle CJ, Shekhar A (2007) From anxiety to autism: spectrum of abnormal social behaviors modeled by progressive disruption of inhibitory neuronal function in the basolateral amygdala in Wistar rats. Psychopharmacology (Berl) 191:107–118.

Varty GB, Cohen-Williams ME, Morgan CA, Pylak U, Duffy RA, Lachowicz JE, Carey GJ, Coffin VL (2002) The gerbil elevated plus-maze II: anxiolytic-like effects of selective neurokinin NK1 receptor antagonists. Neuropsychopharmacology 27:371–379.

Woodruff AR, Sah P (2007a) Inhibition and synchronization of basal amygdala principal neuron spiking by parvalbumin-positive interneurons. J Neurophysiol 98:2956–2961.

Woodruff AR, Sah P (2007b) Networks of parvalbumin-positive interneurons in the basolateral amygdala. J Neurosci 27: 553–563.

Woodson W, Farb CR, Ledoux JE (2000) Afferents from the auditory thalamus synapse on inhibitory interneurons in the lateral nucleus of the amygdala. Synapse 38:124–137.

(Accepted 2 December 2011)
(Available online 24 December 2011)